TU/e EINDHOVEN UNIVERSITY OF TECHNOLOGY

Ultrasonic delay lines for the PAL colour-television system

Citation for published version (APA):
Backers, F. T. (1968). *Ultrasonic delay lines for the PAL colour-television system*. [Phd Thesis 1 (Research TU/e / Graduation TU/e), Applied Physics and Science Education]. Technische Hogeschool Eindhoven. https://doi.org/10.6100/IR161551

DOI:
10.6100/IR161551

Document status and date:
Published: 01/01/1968

Document Version:
Publisher's PDF, also known as Version of Record (includes final page, issue and volume numbers)

Please check the document version of this publication:

• A submitted manuscript is the version of the article upon submission and before peer-review. There can be important differences between the submitted version and the official published version of record. People interested in the research are advised to contact the author for the final version of the publication, or visit the DOI to the publisher's website.
• The final author version and the galley proof are versions of the publication after peer review.
• The final published version features the final layout of the paper including the volume, issue and page numbers.

Link to publication

General rights
Copyright and moral rights for the publications made accessible in the public portal are retained by the authors and/or other copyright owners and it is a condition of accessing publications that users recognise and abide by the legal requirements associated with these rights.

• Users may download and print one copy of any publication from the public portal for the purpose of private study or research.
• You may not further distribute the material or use it for any profit-making activity or commercial gain
• You may freely distribute the URL identifying the publication in the public portal.

If the publication is distributed under the terms of Article 25fa of the Dutch Copyright Act, indicated by the "Taverne" license above, please follow below link for the End User Agreement:

www.tue.nl/taverne

Take down policy
If you believe that this document breaches copyright please contact us at:

openaccess@tue.nl

providing details and we will investigate your claim.

Download date: 07. Nov. 2026

ULTRASONIC DELAY LINES FOR THE PAL COLOUR-TELEVISION SYSTEM

PROEFSCHRIFT

TER VERKRIJGING VAN DE GRAAD VAN DOCTOR IN DE TECHNISCHE WETENSCHAPPEN AAN DE TECHNISCHE HOGESCHOOL TE EINDHOVEN OP GEZAG VAN DE RECTOR MAGNIFICUS, DR. K. POSTHUMUS, HOOGLERAAR IN DE AFDELING DER SCHEIKUNDIGE TECHNOLOGIE VOOR EEN COMMISSIE UIT DE SENAAT TE VERDEDIGEN OP DINSDAG 11 JUNI 1968 DES NAMIDDAGS TE 4 UUR

DOOR

FRANCISCUS THEODORUS BACKERS

NATUURKUNDIG INGENIEUR

GEBOREN TE ROTTERDAM

DIT PROEFSCHRIFT IS GOEDGEKEURD DOOR DE PROMOTOR
PROF. DR. C. ZWIKKER

Aan mijn vrouw

CONTENTS

1. INTRODUCTION 1

2. PURPOSE OF THE PAL DELAY LINE AND REQUIREMENTS TO BE MET 2
   2.1. Outline of the PAL system 2
   2.2. PAL-delay-line requirements 9
   References 25

3. DISCUSSION ON THE PAL DELAY LINE TYPE DL1 AND ON ALTERNATIVE DESIGNS 26
   3.1. Introduction 26
   3.2. Non-ultrasonic delay lines 26
   3.3. Historic survey 27
   3.4. Description of the PAL delay line 30
   3.5. Alternative designs 33
      3.5.1. Attenuation, bandwidth 33
      3.5.2. Delay variation with temperature 35
      3.5.3. Phase-delay accuracy 35
      3.5.4. Dispersion 37
      3.5.5. Conclusion 40
   3.6. The PAL delay line; discussion and results of measurements . . 41
      3.6.1. Attenuation, reflections, bandwidth 41
      3.6.2. Delay variation with temperature 45
      3.6.3. Phase-delay accuracy 47
      3.6.4. Dispersion 48
   References 48

4. DELAY-LINE CHARACTERISTICS 50
   4.1. Theoretical survey 50
   4.2. Approximate examination of transducer-pair responses 57
   4.3. Computations of transfer responses and reflection coefficients . . 62
   4.4. Quantitative data on PXE 3 68
   4.5. Propagation 71
   References 75

5. MEASUREMENTS 76
   5.1. Insertion loss, bandwidth, reflections 76
   5.2. Phase and group delay, temperature stability of phase response, phase adjustment by grinding 77
   References 80

1. INTRODUCTION

This thesis gives an account of a contribution to the design of ultrasonic delay lines encountered in colour-television receivers for one of the two colour-transmission systems introduced in various European countries, the PAL system. These delay lines serve to delay chrominance signals for a period equal to that of a horizontal television scanning line; we shall on occasion find it convenient to refer to them as line delays, to distinguish them from lines having different values of delay. The discussion of the properties of line delays will be kept fairly general; however, the emphasis will be on PAL delay lines wherever practical details are considered, as the author's own experimental investigations in this field have been primarily directed towards the realization of a PAL delay line.

Chapter 2 will be devoted to an examination of the requirements which PAL delay lines should meet. To provide a background for this examination a section will be included giving a brief outline of the transmission system.

The remaining part of this treatise will be devoted to a discussion of the physical and electrical properties of delay lines, which will meet the requirements found in chapter 2, and to a way in which they may be realized in practice.

Chapter 3 gives a general discussion of the delay line which was developed for the purpose. It also examines the relative advantages and disadvantages of alternative designs.

The subjects of wave-propagation and transducer characteristics, which together determine to a large extent the overall electrical characteristics of a delay line, are treated in chapter 4. An exact treatment of problems in these two areas is seldom feasible; usually calculations are based upon one or more assumptions. Therefore, wherever possible, the conclusions of such calculations will be compared with the results of the author's own experiments.

Chapter 5 deals with the methods of measuring various characteristics of delay lines. The PAL delay line is adjusted to the desired delay by grinding away part of the glass propagation body; during this procedure continuous electrical measurements are made on the line. A brief description of this process is included in chapter 5.

2. PURPOSE OF THE PAL DELAY LINE AND REQUIREMENTS TO BE MET

2.1. Outline of the PAL system

This section is intended to provide a background for the discussion on PAL-delay-line requirements in sec. 2.2. For a more complete review of the PAL (Phase Alternation on Lines) transmission system the reader is referred to articles by Bruch [2-1,2]). A survey on the NTSC (National Television System Committee) system, the PAL system and the SECAM (Séquentiel à mémoire) system is given in an article by De Vrijer [2-3]) in which also the relative advantages and disadvantages of the three systems are discussed. Colour-transmission and decoding problems are comprehensively treated by Davidse [2-4]). Here, then, we shall only briefly recapitulate the main features of the PAL system; our notation will be that of De Vrijer [2-3]).

The source of colour-television signals, such as a colour-television camera, delivers the signals R, G and B representing the red, green and blue information in the picture being transmitted. The relation between the luminance of the cathode-ray tube in the receiver and its signal voltage is non-linear; in order to ensure that the relation between the light at the camera and the light output from the receiver is linear for each of the three colours, the signals R, G and B are generally amplified in non-linear amplifiers. The resulting signals ("gamma-corrected signals") are called R', G' and B'. These signals are adjusted to be equal when the corresponding colour in the original scene is white.

Three new signals, Y', S_1 and S_2 are derived from R', G' and B' by linear transformation, as follows:

$$Y' = 0{\cdot}30\,R' + 0{\cdot}59\,G' + 0{\cdot}11\,B', \tag{2.1}$$

$$S_1 = 0{\cdot}88\,(R' - Y'), \tag{2.2}$$

$$S_2 = 0{\cdot}49\,(B' - Y'). \tag{2.3}$$

The luminance signal Y' is analogous to the monochrome signal in monochrome transmission; it is modulated upon the picture carrier as a normal monochrome signal. Its video bandwidth is approximately 5 MHz. The two colour-difference signals S_1 and S_2 are first restricted in bandwidth to approximately 1 MHz; then they are modulated on a subcarrier, the frequency of which is chosen fairly high in the video bandwidth of the luminance signal. The manner of modulation is characteristic of the transmission system; we shall return to this subject shortly.

In the receiver the luminance signal and the colour-difference signals are to be recovered by a decoding technique which is characteristic for the transmission system; subsequently, linear transformation will produce R', G' and B'. If the values of R', G' and B' are equal, then this should result in the reproduction of the colour white on the receiver display tube.

For a linear system, some of the properties of the colour-difference signals are as follows. They are positive, zero or negative. They are both zero for colourless parts of the scene. For a given value of the hue (but not neutral), the magnitudes of the two difference signals increase with the luminance as well as with the saturation. If the system were linear, then the ratio of the two difference signals would be determined by the hue. Real systems are not linear; this modifies the latter property somewhat. The modification is not very significant for the present discussion, however; we can state that the ratio of the two signals is to a large extent determined by the hue.

The description given so far, does not pertain exclusively to the PAL system; it also applies to the NTSC system, as well as to the SECAM system.

In order to clarify the exact purpose and the advantage of the use of a delay line in the PAL system, it is necessary to discuss the reception of the PAL signal in a receiver not equipped with a line delay (PAL-s receiver). It is for this purpose not strictly necessary to discuss the NTSC system. However, since the PAL system is clearly derived from the NTSC system little redundancy is involved in including the main elements of the latter system as well; this we will now proceed to do.

In the NTSC system, the signal S_1 is amplitude-modulated upon the cosine phase of the colour subcarrier; the modulation is performed with a balanced modulator so that the signal $S_1 \cos \omega_s t$ is generated, ω_s being the angular frequency of the colour subcarrier. Similar modulation of S_2 on the sine phase of the same subcarrier results in the signal $S_2 \sin \omega_s t$. The two signals are then added; thus, the resulting signal, which is known as the chrominance signal, is given by

$$C = 0{\cdot}88\,(R' - Y') \cos \omega_s t + 0{\cdot}49\,(B' - Y') \sin \omega_s t.$$

This signal may be represented by either one of the two phasor diagrams of fig. 2.1, where the dashed vectors should be disregarded. Since S_1 and S_2 may be positive, zero or negative, it follows that the phase of the resulting vector C may have any value. Considering the properties of the colour-difference signals S_1 and S_2 noted above, it follows that the phase of the chrominance signal is determined to a large extent by the hue of the colour to be reproduced. Any phase error in the detection will result in a hue error. The phase needs to be measured with respect to some reference phase; in the NTSC system this will be the phase of a reference signal which is transmitted during each horizontal-line-blanking period in the form of bursts of a few cycles of the subcarrier frequency. The reference phase is that of a signal $\sin (\omega_s t - 180°)$ and the receiver is able to regenerate a continuous wave signal from the short bursts. Wherever we use the term phase error in what follows, we mean the error in the phase difference between chrominance signal and reference signal. The phase angle needs to be detected with rather high accuracy, since an error of 5° is

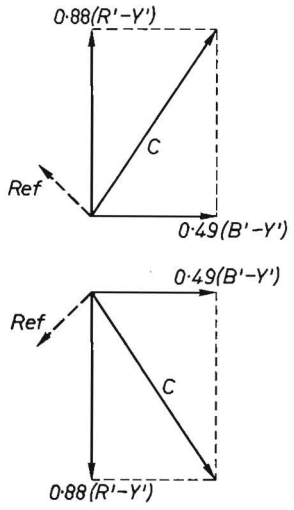


Fig. 2.1. Phasor diagram of the PAL chrominance signal on two consecutive lines.

already noticeable. This phase accuracy is needed in the receiver as well as in every one of the circuits and links leading from studio to receiver. It was the desire to alleviate just this phase sensitivity which stimulated various research and development laboratories in Europe to search for alternative transmission systems. Products of this search include of course the SECAM and, later, the PAL transmission system. We shall now examine how a larger phase tolerance comes about in the PAL system.

In the PAL system, the chrominance signal has the following form:

$$C = \pm 0{\cdot}88\,(R' - Y')\cos\omega_s t + 0{\cdot}49\,(B' - Y')\sin\omega_s t. \qquad (2.4)$$

Here, the $\pm$ symbol is meant to imply that if one sign holds during one horizontal-scanning-line period, the other sign holds during the next line period. This phase-alternation principle constitutes the main difference between the PAL and the NTSC systems. There are other minor differences: for example, the relation between the subcarrier frequency and the horizontal-scanning frequency is different from the corresponding relation in the NTSC system. The reference signal in the PAL system again transmits information regarding the reference phase; but in addition it enables the receiver to decide which of the two types of lines as described by (2.4) is being transmitted.

If we assume the colour-difference signals to be constant during the two successive horizontal-line-scanning intervals n and $n + 1$, the chrominance signal may be represented by the phasor diagram in fig. 2.1.

To reduce the visibility of the subcarrier in the receiver display, its frequency is chosen to satisfy the relation

$$f_s = \left(n - \frac{1}{4}\right) f_L + \frac{1}{625} f_L,$$

where n is a whole number and f_L the line frequency. At the E.B.U. (European Broadcasting Union) conference in Rome in December 1965 the following values were agreed upon:

$$f_L = 15625 \text{ Hz}$$

making the line period 64 μs, and

$$n = 284. \tag{2.5}$$

It follows that

$$f_s = 4{\cdot}4\ 3361875 \text{ MHz}.$$

The complete video signal, consisting of the luminance signal Y', the modulated subcarrier (2.4), synchronization signals, and A.B. (see below) is modulated upon the picture carrier; filtering then takes place, so that frequency components higher than 5 MHz are cut off. Thus the chrominance bandwidth extends from 3·4 to 5 MHz.

The reference signal is represented in fig. 2.1 by the two dashed arrows; these are short wave trains of the subcarrier frequency which are transmitted during the horizontal-line-blanking periods and whose phase is alternately given by $\sin(\omega_s t - 135°)$ and $\sin(\omega_s t - 225°)$. These wave trains, generally referred to as alternating burst (A.B.) enable the receiver to regenerate the carriers $\sin \omega_s t$ and alternatingly $\pm \cos \omega_s t$.

Normal operation of the PAL-s receiver may be described as follows. The receiver is equipped with two synchronous demodulators: the S_1 and the S_2 demodulators. The action of the latter demodulator is effectively the multiplication of the chrominance signal C by $\sin \omega_s t$, which the receiver has regenerated from the A.B. Similarly the product $\pm C \cos \omega_s t$ is formed in the S_1 demodulator, the plus sign being used whenever the plus sign holds in (2.4). As a result, we normally have

$$\begin{aligned} &\text{output of } S_1 \text{ demodulator } +\tfrac{1}{2} S_1\{\cos \quad 2\omega_s t + 1\}, \\ &\text{output of } S_2 \text{ demodulator } +\tfrac{1}{2} S_2\{-\cos 2\omega_s t + 1\}. \end{aligned}$$

After removal of the second-harmonic components, by filtering, the low-frequency components S_1 and S_2 are left, so that the purpose of resolving C into its components S_1 and S_2 has been accomplished.

In the presence of a phase error $\Delta\varphi$, we may put

$$C = \pm S_1 \cos(\omega_s t - \Delta\varphi) + S_2 \sin(\omega_s t - \Delta\varphi),$$

the reference signals still being $\sin \omega_s t$ and $\pm \cos \omega_s t$. The results of demodulation — omitting second harmonics — now give:

for the "plus lines"

S_1 output: $\frac{1}{2}\{S_1 \cos \Delta\varphi - S_2 \sin \Delta\varphi\}$,
S_2 output: $\frac{1}{2}\{S_1 \sin \Delta\varphi + S_2 \cos \Delta\varphi\}$,

and for the "minus lines"

S_1 output: $\frac{1}{2}\{\ S_1 \cos \Delta\varphi + S_2 \sin \Delta\varphi\}$,
S_2 output: $\frac{1}{2}\{-S_1 \sin \Delta\varphi + S_2 \cos \Delta\varphi\}$.

If we consider the signal on a "plus line", we notice that its S_1/S_2 ratio is wrong: a hue error has been introduced. This error is of course identical with the NTSC hue error. There is a hue error in the minus lines also, but this error is in the opposite direction: if on one line the hue were too blue, on the next line it would be not blue enough. If in some way we could add the corresponding outputs of two lines in succession (we are disregarding vertical transitions in the picture), we would obtain

S_1 output: $S_1 \cos \Delta\varphi$,
S_2 output: $S_2 \cos \Delta\varphi$.

In this case the ratio S_1/S_2 and thus the reproduced hue would be correct; there would be a reduction in the amplitude of the colour-difference signals, but for reasonable values of $\Delta\varphi$ the corresponding reduction in colour saturation would be quite acceptable.

The question now is how this summation can be realized. The philosophy behind PAL-s reception is that the addition will be accomplished by the eye, which, at a certain viewing distance, will not resolve the separate lines. Although it is somewhat simplistic to say that the eye adds the output signals of the demodulators, nevertheless if one examines in detail what happens if the eye adds the light coming from two adjoining lines in the display, then one finds that at least for the linear approximation, the reproduced and summated light has the correct hue.

Unfortunately the visual summation is far from ideal. There are several reasons for this. In the first place two lines which are successive in time are not adjoining lines in the picture, due to the interlacing technique. The resulting structure — known as Hannover Bars — is twice as coarse as the line structure of a black-and-white picture. Due to the non-linearity of the system, the hue errors are accompanied by luminance errors which usually serve to increase the visibility of the effect. A third effect, and perhaps the most important one, is the apparent upward crawl which the Hannover Bars show. This crawl is also caused by the interlacing technique and its speed is low enough to be followed by the eye. In fact, in large uncluttered picture areas the eye often has a tendency to follow the upward movement quite closely. Apart from the fact that the effect is quite noticeable, it should be noted that integration by

the eye is effectively combated by the eye's following of the crawl. There is, in fact, some experimental evidence supporting this view. If an observer looks at the Hannover Bars through an opaque screen containing a hole just large enough so that the observer sees just four lines, the phase tolerance is much increased *). Also the visibility of Hannover Bars is less in cluttered picture areas.

The summation by eye, then, is often incomplete and leads to undesirable picture degradations. The purpose of including a PAL delay line in a PAL receiver is to ensure correct summation or "averaging" of the chrominance information of two consecutive horizontal lines, which, as was shown before, is needed to ensure the reproduction of correct hues in the presence of phase errors. The aim, then, is to do the averaging by means of a line delay, so that its effectiveness is not a function of the viewing distance. A further but not essential difference is that the averaging by delay line is performed before demodulation. We now turn to a brief description of the process of decoding with the aid of a delay line.

Figure 2.2 shows a block diagram of a typical decoder circuit for a PAL-d receiver. The gate shown in fig. 2.2 is controlled by horizontal synchronization pulses in such a way as to direct the alternating burst and the chrominance signals in the directions shown. The chrominance signal then enters the part of the circuit shown within the dashed lines. It is seen that the delayed signal $C_{n\tau}$ is added to and subtracted from the undelayed signal C_{n+1}.

Ideally the delay line has the following properties:

(a) the group delay of the delay line equals T_L (T_L = the period of a horizontal scanning line = 64 μs);
(b) the phase response for the subcarrier frequency equals an integral number times 2π;
(c) the delay line has constant attenuation within the chrominance bandwidth.

The attenuation in the undelayed path (fig. 2.2) is set equal to the attenuation of the delay line.

For a delay line with these properties, it will be deduced in the next section that the addition and the subtraction of delayed and undelayed signals produce the signals $\pm 2\times 0{\cdot}88\,(R'-Y')\cos\omega_s t$ and $2\times 0{\cdot}49\,(B'-Y')\sin\omega_s t$, provided that

$$S_1(t) = S_1(t-T_L) \quad \text{and} \quad S_2(t) = S_2(t-T_L). \tag{2.6}$$

That this is so can be made plausible by means of fig. 2.1; if the delay line has the given properties, then the two signals represented by the diagram of this figure are simultaneously available.

*) Private communication by Mr L. A. J. M. Verhoeven.

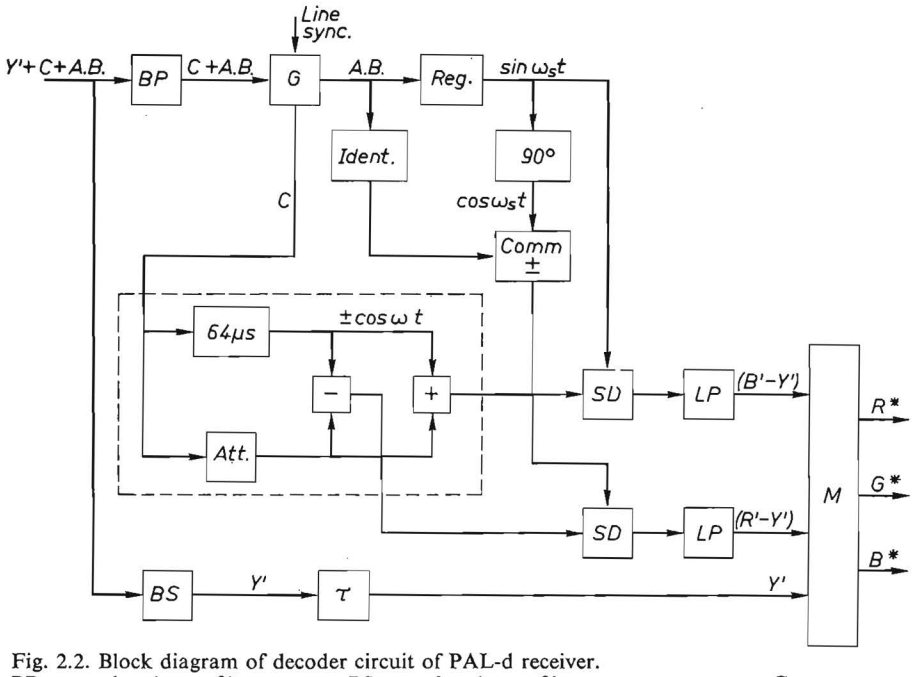


Fig. 2.2. Block diagram of decoder circuit of PAL-d receiver.

BP	= band-pass filter,	BS	= band-stop filter,	G	= gate,
Reg	= regenerator,	Ident	= identification circuit,	M	= matrix,
Comm	= commutator,	SD	= synchronous demodulator,		
LP	= low-pass filter,	T	= equalizing delay line,		
Att	= attenuator,	64 μs	= line delay,		
A.B.	= alternating burst	C	= chrominance signal.		

The chrominance signal has now been resolved into its two components although the vertical component still alternates, line-sequentially, in polarity. The two components are then operated upon by the synchronous detectors shown in fig. 2.2; this operation may mathematically be described as multiplication of the two signals by $\pm \cos \omega_s t$ and $\sin \omega_s t$, respectively. The detector outputs, therefore, contain the colour-difference signals themselves and components of twice the carrier frequency. The latter components are removed in the low-pass filters.

The generation of the signals $\pm \cos \omega_s t$ and $\sin \omega_s t$ needed for the synchronous demodulators is also indicated schematically in fig. 2.2. The sine phase of the carrier is produced by the regenerator. From this phase the cosine phase is derived. The polarity of the latter signal is line-sequentially alternated in a commutator circuit. To obtain the correct sequence of alternation this commutator is controlled by an identification circuit which in turn receives its information from the alternating burst.

The luminance signal is obtained by removing the chrominance information from the incoming video signal by means of a band-stop filter. It is then de-

layed, to equalize its delay with that of the chrominance signals. The delay needed for this purpose is generally a fraction of a microsecond; it is obtained in an electromagnetic delay line. Finally the signals Y', $(R' - Y')$ and $(B' - Y')$ are linearly transformed by the matrix M into the signals R^*, G^* and B^*, which, for frequencies up to approximately 1 MHz, are equal to R', G' and B'.

So far it has been assumed (eq. (2.6)) that at the time $t + 64\ \mu s$, the colour-difference signals were not appreciably different from the corresponding signals at the time t. For a very large percentage of the time this assumption is justified. It is invalid, of course, wherever a sharp vertical colour transition occurs; in such a case (2.4) still holds, but the addition and subtraction of undelayed and delayed signals in the receiver produces an averaging effect. The location of the reproduced hue in the chrominance diagram may then be found by addition of the two vectors representing the chrominance before and after the vertical transition. Due to the interlacing technique this intermediate colour will appear on the two horizontal lines immediately following the transition.

It is not our purpose in this section to discuss the various advantages and disadvantages of the PAL system as compared, for example, with the NTSC system. We should like to mention however that the advantages cannot be fully gained if the properties of the delay line in the PAL-d receiver are not held within rather close tolerances, which we shall attempt to determine in the next section. For example it is well known [2-1,3]) that the PAL system allows a larger overall differential phase error, provided the signal is received with a PAL-d receiver. It is also known [2-1]) that departures from the ideal phase and amplitude characteristics in the PAL system do not lead to cross-talk from one colour-difference channel into the other (quadrature cross-talk), provided again that the receiver has a delay-line decoder. These two statements are no longer valid if the phase and amplitude characteristics of the delay line are not within the required tolerances. Moreover, a deficient delay line will produce additional picture degradations, which are generally of a different nature from those which the PAL system was designed to eliminate.

2.2. PAL-delay-line requirements

Required phase response at the subcarrier frequency

The desired phase response of the delay line for the colour-subcarrier frequency will be found from the requirement that pictures of homogeneous hue and luminance ("large-area colours") shall be reproduced correctly. We have

$$S_1 = 0{\cdot}88\,(R' - Y')$$

and

$$S_2 = 0{\cdot}49\,(B' - Y').$$

In this case S_1 and S_2 are independent of time. The chrominance signal on

two successive lines n and $n + 1$ may be written:

$$C_n = \pm S_1 \cos \omega_s t + S_2 \sin \omega_s t, \tag{2.7}$$

and

$$C_{n+1} = \mp S_1 \cos \omega_s t + S_2 \sin \omega_s t. \tag{2.8}$$

The output of the delay line whose input is C_n will be

$$C_{n\tau} = \pm S_1 \cos (\omega_s t - \beta_s) + S_2 \sin (\omega_s t - \beta_s), \tag{2.9}$$

where β_s is the phase response of the delay line for the subcarrier frequency. If we require that

$$C_{n\tau} + C_{n+1} = 2 S_2 \sin \omega_s t \tag{2.10}$$

and

$$C_{n\tau} - C_{n+1} = \pm 2 S_1 \cos \omega_s t, \tag{2.11}$$

the equations (2.10) and (2.11) are satisfied if β_s has any one of the values

$$\beta_s = 2 m\pi, \tag{2.12}$$

where m may be any integer.

Here we have assumed that the attenuation of the delay line is zero for f_s. In actual practice the amplitudes will be made equal by attenuating the undelayed signals. Demodulation corresponding to (2.10) and (2.11) will be as follows:

blue-difference channel: $(C_{n\tau} + C_{n+1}) \sin \omega_s t$, (2.13)

red-difference channel: $(C_{n\tau} - C_{n+1}) (\pm \cos \omega_s t)$. (2.14)

In the present case S_2 and S_1 are constant, giving

$$(C_{n\tau} + C_{n+1}) \sin \omega_s t = S_2 + \text{second-harmonic term},$$
$$(C_{n\tau} - C_{n+1}) (\pm \cos \omega_s t) = S_1 + \text{second-harmonic term}.$$

The second-harmonic terms are filtered out, as mentioned in the previous section.

The requirements (2.10) and (2.11) are rather arbitrarily chosen. For example we could have required

$$C_{n\tau} + C_{n+1} = \mp 2 S_1 \cos \omega_s t \tag{2.15}$$

and

$$C_{n\tau} - C_{n+1} = -2 S_2 \sin \omega_s t, \tag{2.16}$$

which would have led to

$$\beta_s = m\pi, \tag{2.17}$$

and to the following demodulation:

blue channel: $(C_{n\tau} + C_{n+1}) (\mp \cos \omega_s t)$, (2.18)

red channel: $(C_{n\tau} - C_{n+1})(-\sin \omega_s t)$. (2.19)

With regard to the receiver design, this requirement is not very different from the previous one; the only consequences are: the two output connections from the dashed section in fig. 2.2 need to be interchanged and the polarities of the demodulator-reference signals need to be reversed. Since it has become customary to state that the sum of delayed and undelayed signals produces the blue-difference information (2.10), the reader may well ask why the possibility of another requirement should be mentioned at all. Our reason for bringing it up is that a priori there is the possibility that the phase requirement (2.17) might be more suitable for the design of the delay line. It should be remembered that the delay line must give not only the correct phase response but also the correct group delay. Starting with a design giving $2\,m\pi$ phase response and a certain group delay it is conceivable that a reduction of the length of the propagation medium will result in a $(2m - 1)\pi$ phase response together with a group delay which more closely approximates to the required group delay. If the output of the delay line is balanced, or if balanced transformers are used in input or output, this matter really becomes trivial. We shall continue therefore to employ the more conventional requirements (2.10)-(2.14) keeping in mind that the phase response (2.17) is also acceptable.

Required amplitude and phase-frequency characteristics

Input undistorted

We again write the chrominance signals in successive lines as in (2.7) and (2.8) but S_1 and S_2 are no longer considered constant. The required amplitude and phase-frequency responses are easily found by noting that the response to a signal $G(t)\cos(\omega_s t - \varphi)$ of a device with idealized-network-response characteristics will be $G(t - T)\cos(\omega_s t - \varphi)$. Here $G(t)$ represents an arbitrary signal containing frequencies up to f_m, and φ is any constant phase; by "idealized network response" is meant the response shown in fig. 2.3. The phase characteristic is a straight line in the frequency range from $f_s - f_m$ to $f_s + f_m$ and having a slope of T s; for the frequency f_s, β has the value $2\,m\pi$. The amplitude response is constant over the same range of frequencies. It is clear then, that if we choose for the delay line an idealized-network response, with f_s as central frequency and with the slope of the phase response equal to the horizontal-line period T_L (= 64 μs), the requirements (2.10) and (2.11) will again be satisfied, provided of course that $S_1(t - T_L) = S_1(t)$ and $S_2(t - T_L) = S_2(t)$.

The ideal delay-line-phase response, then, is as shown in fig. 2.3; as m is unspecified there is a family of acceptable responses, to which may be added those straight line-phase responses with $\beta_s = m\pi$ and slope T_L. The line $\beta = \omega T_L$ is not one of these, as can be seen by substituting the chosen colour-

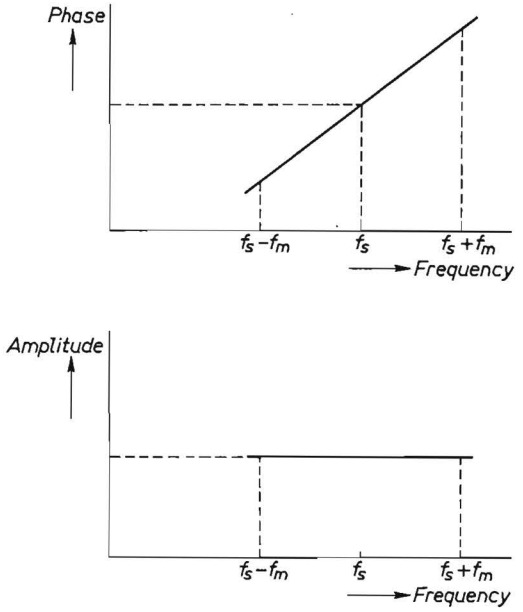


Fig. 2.3. Idealized-network response.

subcarrier frequency given in sec. 2.1. The foregoing may be summarized as follows: the envelope of the modulated chrominance signal is delayed by a line period since the group delay of the delay line is chosen equal to the line period, while the carrier phases of delayed and undelayed signals are made respectively of equal and of opposite polarity, by adherence to the phase relations (2.12) and (2.17).

Required amplitude and phase-frequency characteristics

Input distorted

It might not be very realistic to assume that the chrominance signal will be transmitted from the transmitter to the PAL decoder in the receiver without suffering amplitude or phase distortion. We shall therefore first examine what the results will be if a delay line, having the idealized network response discussed in the previous subsection, is used in conjunction with an input signal which has undergone linear amplitude and phase distortion. After that we shall briefly investigate the feasibility of deliberately departing from the idealized-network characteristics with the purpose of correcting the input distortions.

We will assume that a variable red-difference signal S_1 is being transmitted:

$$S_1 = \int_0^{\omega_m} S_1(\omega) \cos \{\omega t - \phi(\omega)\} d\omega. \tag{2.20}$$

After modulation, this becomes

$$S_1 \cos \omega_s t = \tfrac{1}{2} \int_0^{\omega_m} [S_1(\omega) \cos \{(\omega_s + \omega)t - \phi(\omega)\} + \\ + S_1(\omega) \cos \{(\omega_s - \omega)t + \phi(\omega)\}]d\omega. \qquad (2.20a)$$

Distortion then results in the following signal at the input of the delay line:

$$\text{input} = \tfrac{1}{2} \int_0^{\omega_m} [\alpha_U(\omega)S_1(\omega) \cos \{(\omega_s + \omega)t - \phi(\omega) - \psi_U(\omega)\} + \\ + \alpha_L(\omega)S_1(\omega) \cos \{(\omega_s - \omega)t + \phi(\omega) - \psi_L(\omega)\}]d\omega, \qquad (2.21)$$

where $\alpha_U(\omega)$, $\alpha_L(\omega)$, $\psi_U(\omega)$ and $\psi_L(\omega)$ are the transmission amplitude and phase responses for the upper and lower side-bands.

The output of the idealized-network delay line will be

$$\text{output delay line} = \tfrac{1}{2} \int_0^{\omega_m} [\alpha_U(\omega)S_1(\omega) \cos \{(\omega_s + \omega)t - \omega T_L - \phi(\omega) - \psi_U(\omega)\} + \\ + \alpha_L(\omega)S_1(\omega) \cos \{(\omega_s - \omega)t + \omega T_L + \phi(\omega) - \psi_L(\omega)\}]d\omega. \qquad (2.22)$$

If we repeat the procedure (2.20)-(2.21), starting with a signal $S_1'(t) = S_1(t - T_L)$, the input signal (2.21) will be identical with the expression (2.22). This means that for all those instances when $S_1(t - T_L) = S_1(t)$ (and other instances are not under consideration) we shall obtain complete cancellation by adding input and output signals. In other words, there will be no cross-talk from the red- into the blue-difference channel. Subtraction gives the original signal, so that the original distortion still exists. A similar derivation for the blue-difference signal gives the corresponding result.

Before accepting the idealized-network characteristics as the best characteristics for the purpose it might be asked if delay-line characteristics cannot be chosen in such a manner that the distortion in the input signal is eliminated. Calculation shows that it is in general not possible to obtain complete compensation of the original distortion without simultaneous reapparance of blue information in the red channel and vice versa. It is, at least in theory, possible to obtain compensation of the input distortion in such a manner that the cross-talk will only have a component perpendicular to the particular synchronous-demodulation axis. In the absence of demodulation phase errors, this would mean that effectively no cross-talk would be present. The question remains, of course, whether the delay-line characteristics so determined could actually be realized. In fact the distortion of the chrominance signal is not really a known quantity since it may be influenced to an appreciable extent by the user of the receiver when he tunes in on the station selected. Furthermore it may be said that the elimination of quadrature cross-talk is a much more desirable goal than the complete elimination of the amplitude and phase distortion which are to be

expected in PAL receivers; a rather extreme example of cross-talk is given by Brùch [2-2]).

The delay line with idealized-network characteristics will eliminate cross-talk independently of the setting of the fine tuning control even when demodulation is not perfect. We shall therefore pursue the possibility of distortion compensation no longer, and assume that the idealized-network characteristics give the most favourable response. We turn now to the task of determining the tolerances allowable in these characteristics.

Tolerance in phase response at the subcarrier frequency

Figure 2.4 depicts the decoding process during two successive lines. The first column shows the transmitted chrominance signal which is assumed constant. The output of the delay line is given in the second column; the phase response is assumed to be $\Delta\beta_s$ degrees different from $2\pi m$, so that the chrominance vector C' is produced instead of C. The third column then shows addition and subtraction of delayed and direct signals; it also shows the demodulation of the

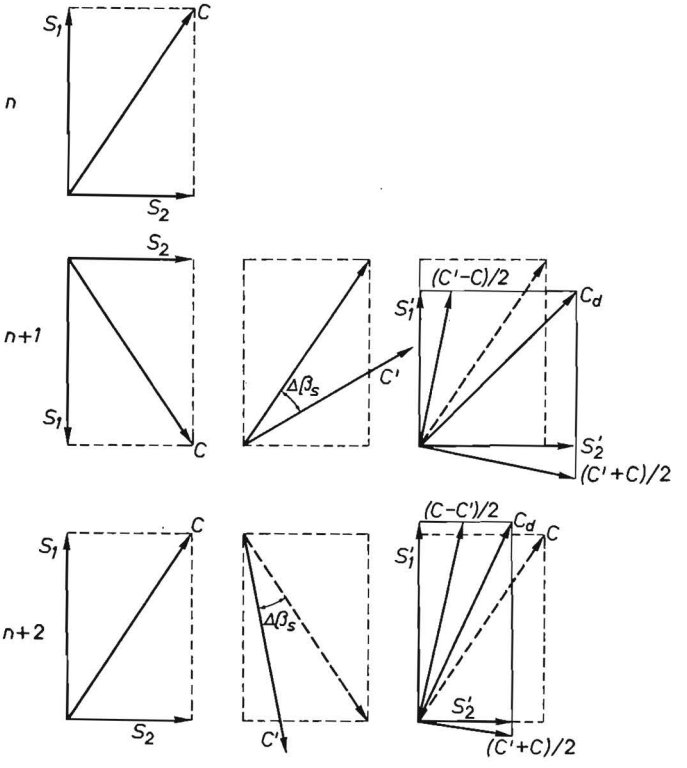


Fig. 2.4. Delay-line-phase-response error $\Delta\beta_s$ at subcarrier frequency. First column: input signal, second column: delayed signal, third column: summation and subtraction; chrominance after detection is represented by C_d.

sum signals and of the difference signals in the S_2 and in the S_1 direction, respectively. The demodulation products are called S_2' and S_1' and the vector having S_2' and S_1' as components is called C_d. Solving the problems of trigonometry involved, we find

$$|C_d| = (\cos \Delta\beta_s)|C| \tag{2.23}$$

and

$$\varphi' - \varphi = \pm \Delta\beta_s/2, \tag{2.24}$$

where

$$\tan \varphi = S_1/S_2$$

and (2.25)

$$\tan \varphi' = S_1'/S_2'.$$

The visible effect of this error is identical with the effect which the PAL receiver without delay line will show if a phase error of $\Delta\beta_s/2$ obtains.

The actual value of $\Delta\beta_s$ where the effects are just noticeable have been determined by experiment. It is difficult to be very precise in this respect; most observers agree that the tolerance in the phase error is approximately $\pm$ 12°.

Tolerance in phase-frequency characteristics

We assume undistorted transmission. First let a red-difference signal varying sinusoidally with the modulation frequency $p/2\pi$ be transmitted. The input chrominance signal is thus given by (2.7) and (2.8) with $S_2 = 0$ and $S_1 = S_{1m} \cos pt$.

Demodulation is performed according to (2.13) and (2.14). We define

$$\Delta\beta = \beta - \beta_0, \tag{2.26}$$

$$\beta_0 = 2\pi m + pT_L, \tag{2.27}$$

where β is the actual phase-frequency response, β_0 the desired idealized-network phase response, T_L the horizontal-line period and $\Delta\beta$ the deviation from the desired phase response. We now make the further assumption that all modulation frequencies $p/2\pi$ will be multiples of the line frequency; this means that we do not consider changes in the vertical direction of the scene. With these assumptions we have

$$C_n = \pm [\tfrac{1}{2}S_{1m} \cos (\omega_s + p)t + \tfrac{1}{2}S_{1m} \cos (\omega_s - p)t], \tag{2.28}$$

$$C_{n\tau} = \pm \tfrac{1}{2}S_{1m}[\cos \{(\omega_s + p)t - \Delta\beta(p)\} + \cos \{(\omega_s - p)t - \Delta\beta(-p)\}], \tag{2.29}$$

$$C_{n+1} = \mp \tfrac{1}{2}S_{1m}[\cos (\omega_s + p)t + \cos (\omega_s - p)t]. \tag{2.30}$$

Demodulation according to (2.13) and (2.14) and subsequent filtering of the second harmonics, when carried out for the upper-sideband frequency only, will result in:

blue-difference-channel output =

$$\pm \tfrac{1}{4}S_{1m} \sin pt \mp \tfrac{1}{4}S_{1m} \sin \{pt - \Delta\beta(p)\}, \tag{2.31}$$

red-difference-channel output =

$$\tfrac{1}{4}S_{1m} \cos pt + \tfrac{1}{4}S_{1m} \cos \{pt - \Delta\beta(p)\} \tag{2.32}$$

or:

blue-difference-channel output =

$$\pm \tfrac{1}{2}S_{1m} \sin \{\Delta\beta(p)/2\} \cos \{pt - \Delta\beta(p)/2\}, \tag{2.33}$$

red-difference-channel output =

$$\tfrac{1}{2}S_{1m} \cos \{\Delta\beta(p)/2\} \cos \{pt - \Delta\beta(p)/2\}. \tag{2.34}$$

By substituting $-pt$ for pt we find the output for the lower-sideband frequency; thus
blue-difference-channel output =

$$\pm \tfrac{1}{2}S_{1m} \sin \{\Delta\beta(-p)/2\} \cos \{pt + \Delta\beta(-p)/2\}, \tag{2.35}$$

red-difference-channel output =

$$\tfrac{1}{2}\, S_{1m} \cos \{\Delta\beta(-p)/2\} \cos \{pt + \Delta\beta(-p)/2\}. \tag{2.36}$$

The phase deviation may be divided into an odd part $\Delta\beta_1$ and an even part, $\Delta\beta_2$, as follows:

$$\Delta\beta = \Delta\beta_1 + \Delta\beta_2, \tag{2.37}$$

where

$$2\,\Delta\beta_1 = \{\Delta\beta(p) - \Delta\beta(-p)\}, \tag{2.38}$$

$$2\,\Delta\beta_2 = \{\Delta\beta(p) + \Delta\beta(-p)\}. \tag{2.39}$$

Assuming that the phase deviation consists of an odd contribution $\Delta\beta_1$ only, and considering the two sidebands together, demodulation and filtering will give

$$\text{blue-difference-channel output} = 0, \tag{2.40}$$

red-difference-channel output =

$$S_{1m} \cos \{\Delta\beta_1(p)/2\} \cos \{pt - \Delta\beta_1(p)/2\}. \tag{2.41}$$

It follows that this type of phase deviation in conjunction with an undistorted input will give no quadrature cross-talk and thus no hue change. There will be a saturation loss $\cos(\Delta\beta_1/2)$ and a delay of $\Delta\beta_1(p)/2$.

If the phase deviation consists of $\Delta\beta_2$ only we will have

blue-difference-channel output =

$$\pm S_{1m} \sin \{\Delta\beta_2(p)/2)\} \cos \{\Delta\beta_2(p)/2\} \cos pt, \tag{2.42}$$

red-difference-channel output =

$$S_{1m} \cos^2 \{\Delta\beta_2(p)/2\} \cos pt. \tag{2.43}$$

An even phase deviation, then, will give no delay, assuming again an undistorted input; however a hue change will be produced, corresponding to a rotation through an angle $\Delta\beta_2/2$ in the S_1,S_2 diagram. Also a saturation loss of $\cos(\Delta\beta_2/2)$ occurs and, last but not least, the hue change alternates in polarity.

All conclusions would have been analogous had we included a blue-difference signal of modulation frequency $p/2\pi$; therefore this complication will not be included here. A general phase deviation consisting of the sum of $\Delta\beta_1$ and $\Delta\beta_2$ will give effects which are approximately equal to the sum of the effects of $\Delta\beta_1$ and $\Delta\beta_2$ separately. In this case the output for the red-difference variation considered so far, and for undistorted input may be found by substituting

$$\Delta\beta(p) = \Delta\beta_1 + \Delta\beta_2 \tag{2.44}$$

and

$$\Delta\beta(-p) = -\Delta\beta_1 + \Delta\beta_2 \tag{2.45}$$

in the equations (2.33) and (2.34) or in (2.35) and (2.36). The result is:
blue-difference-channel output =

$$\pm \tfrac{1}{2} S_{1m} \cos(pt - \Delta\beta_1) \sin \Delta\beta_2, \tag{2.46}$$

red-difference-channel output =

$$\tfrac{1}{2} S_{1m} [\cos pt + \cos(pt - \Delta\beta_1) \cos \Delta\beta_2]. \tag{2.47}$$

The output thus describes an ellipse in the S_1,S_2 diagram. The small axis of this ellipse is so small, however, that we may approximate it by a straight line going through the origin and making an angle of $\Delta\beta_2/2$ with the S_1 axis; this same approximation shows the output to be delayed by $\Delta\beta_1/2$. We would also have obtained this approximate result simply by adding the effects of (2.40) to (2.43). It might be argued that the approximation is not very good near the origin since at the moment when (2.46) is zero, (2.47) gives a small output which represents a temporary hue change of 90°. However, the output of (2.47) is at that moment very small even if the amplitude S_{1m} is as large as possible; thus this error represents a temporary deviation from the colour white, for which of course the actual angle in the S_1,S_2 diagram is not of great interest.

Having discussed the various effects of phase deviations, there remains the task of deciding on tolerance values for $\Delta\beta$. Although the theoretical discussion

of errors may aid our understanding of the matter, the final decision on the errors that are just tolerable must still be determined by experiment. Unfortunately we do not have as much experimental evidence regarding the sideband tolerance as we do with respect to the phase error at the subcarrier frequency. Lacking sufficient experimental background we shall base our estimates of the tolerances on two theoretical criteria.

First, we have seen that the even contribution $\Delta\beta_2$ causes hue changes which alternate in polarity on successive lines. It is perhaps reasonable therefore to require for $\Delta\beta_2$ the same tolerance as for the phase response at the subcarrier frequency, as the effects are similar. Thus $\Delta\beta_2$ should be within plus or minus 12° from the value β_0 within the entire chrominance bandwidth. Experience with laboratory receivers having undistorted chrominance input indicates that this requirement gives very good results indeed, although in the author's opinion it is desirable to allow less tolerance at the colour subcarrier, especially since this higher precision can be obtained at reasonable cost. It is not impossible, on the other hand, that the requirement for the sidebands may be relaxed, perhaps by a factor of two or three for the higher modulation frequencies. Also an additional phase ripple due to reflections is allowable; this ripple may be added to the stated tolerance limits as long as the original tolerance for the phase deviation at the subcarrier frequency is not exceeded. Reflections will be discussed in the next subsection.

The odd phase-deviation component $\Delta\beta_1$ is mainly responsible for delay in the colour transitions. It is probably quite reasonable to require this delay to be within the same bounds as required in the NTSC system for the mutual delay between the chrominance signal and the luminance signal. This would, according to the foregoing discussion, lead to the requirement that $\frac{1}{2}\mathrm{d}\beta_1/\mathrm{d}\omega$ shall be within $\pm$ 50 ns within the entire bandwidth. It is to be realized, however, that a similar delay tolerance already exists elsewhere in the receiver so that it would be better to make this tolerance a factor of 2 more severe; thus, the slope of the β_1 vs ω curve should be within $\pm$ 50 ns from 64·000 μs within the chrominance bandwidth. Here it is especially important to add the stipulation that phase ripple is allowable since otherwise the slope requirement for β_1 will be unnecessarily severe.

The division of β into an even and an odd part becomes less meaningful the more the original input signal becomes asymmetric. For the extreme case of single-sideband input the equations (2.35) and (2.36) may be used to calculate responses. A treatment of this case would lead us rather far afield in receiver-design problems and the results obtained would not represent the reality. Fortunately the input will not be single-sideband; except for the higher modulation frequencies it will probably be reasonably symmetric. We shall assume therefore that the given tolerance requirements will still be sufficient for the input asymmetry to be expected in future receivers.

Reflections

The energy which is transmitted through the delay line will, for several reasons, generally not be fully absorbed in the electrical load on the output side. The non-absorbed part may be reflected towards the input side and so on. Thus if an r.f. pulse is transmitted at time $t = 0$ a reflected pulse may be found at the input at the time $t = 2\,T_L$ and another reflected pulse may arrive at the output at the time $t = 3\,T_L$. We shall refer to such pulses as 2τ and 3τ reflections. The term 2τ reflection is meant to indicate that its arrival occurs $2\,T_L$ seconds after $t = 0$, not that its arrival is necessarily on the input side. In fact the folded-delay-line design discussed later receives a small amount of 2τ reflections on its output load. Since this reflection is rather small we shall discuss here mainly the 3τ reflection. Our point of departure will be the tolerance value for this reflection as found by experiment. We will then translate this finding into a tolerance requirement for the phase and amplitude ripples. First, however, it should be pointed out that the 3τ reflections need not bother us in the large-area colours *), as long as the phase adjustment of the delay line at the subcarrier frequency is carried out with a continuous wave input. In that case all the reflections will be included in the phase response and no ill effects can occur within large-area colours.

In or after transitions, however, 3τ reflections could be visible. Experiments show that these reflections are fairly tolerable. For the 3τ reflection, suppression of 26 dB with respect to the output signal seems to be entirely satisfactory; 23 dB is quoted by some observers as representing the tolerable limit. Let the 1τ output for the frequency $\omega/2\pi$ be given by

$$\cos\{\omega(t - T_L) - \varphi\}. \tag{2.48}$$

Assume that the extra phase difference for the 3τ reflection is $2\omega T_L$; this is not necessarily exact, but it will be sufficiently accurate for our purpose. Then the 3τ output will be given by

$$\varepsilon \cos\{\omega(t - 3\,T_L) - \varphi\}. \tag{2.49}$$

Disregarding other reflections, the total output will be

$$(1 + \varepsilon^2 + 2\varepsilon \cos 2\omega T_L)^{1/2} \cos\{\omega(t - T_L) - \varphi - \psi\}, \tag{2.50}$$

where

$$\psi = \arctan \frac{\varepsilon \sin 2\omega T}{1 + \varepsilon \cos 2\omega T}. \tag{2.51}$$

If we vary ω (staying within the chrominance bandwidth), φ will vary only slowly, and to a small extent, from the constant value which it should ideally

*) Unfortunately this is not true for 2τ reflections.

have. Therefore ψ may be considered to be the ripple which was mentioned before. For small values of ε, ψ may be approximated by

$$\psi = \varepsilon \sin 2\omega T_L. \tag{2.52}$$

Thus, the "period" of the ripple in the phase-frequency characteristic is

$$\Omega = \pi/T_L, \tag{2.53}$$

corresponding to a frequency interval of approximately 7·8 kHz. The maximum slope of the phase ripple follows from (2.52):

$$\left(\frac{d\psi}{d\omega}\right)_m = 2T_L\varepsilon. \tag{2.54}$$

Substituting 64 μs for T_L and 0·05 for ε (26 dB suppression) it is found that

$$\left(\frac{d\psi}{d\omega}\right)_m = 6{\cdot}4 \text{ μs},$$

which is very much more than the 50 ns deduced for the tolerance in $d\beta_1/d\omega$, and yet we know that a 5% reflection is tolerable. The tolerance on $d\beta_1/d\omega$ then should be interpreted as applying to the average value of $d\beta_1/d\omega$. Actually, if the assumption concealed in (2.49) is sufficiently accurate and if we adjust the delay line so that $(\varphi - \psi)$ in (2.50) is zero for ω_s, then the contribution of the phase ripple ψ is zero for all modulation frequencies which are a multiple of 15625 Hz. Therefore we may expect that the reflections will cause very little visible effect in the horizontal transitions. The main effect of reflections then should be the prolongation of vertical transitions.

Using 26 dB as an acceptable value of the suppression of 3τ reflections, eq. (2.50) shows that the *p-p* (peak-to-peak) value of the amplitude ripple may be 10% of the average output amplitude; the tolerance on the *p-p* value of the phase ripple is 5·7°, as follows from (2.52). An example of a phase-frequency characteristic which meets all the foregoing requirements is shown in fig. 2.5.

2τ reflections

Very briefly we shall discuss now the subject of 2τ reflections, not with the object of determining the requirements in this respect, but rather to illustrate the effects which they cause in large-area colours.

We assume that the 2τ reflection is the only undesired response in the delay line. We further assume that phase and amplitude adjustment of the line is carried out in such a manner that a correct response is obtained for colours having only a $(B' - Y')$ component. This means that if the input equals $\sin \omega_s t$ then the output of the line is also given by $\sin \omega_s t$. Figure 2.6*a* shows the two components 1τ and 2τ (with the respective amplitudes ϱ_1 and ϱ_2) and their resultant $\sin \omega_s t$. The angle ϑ is the phase difference (omitting an integral

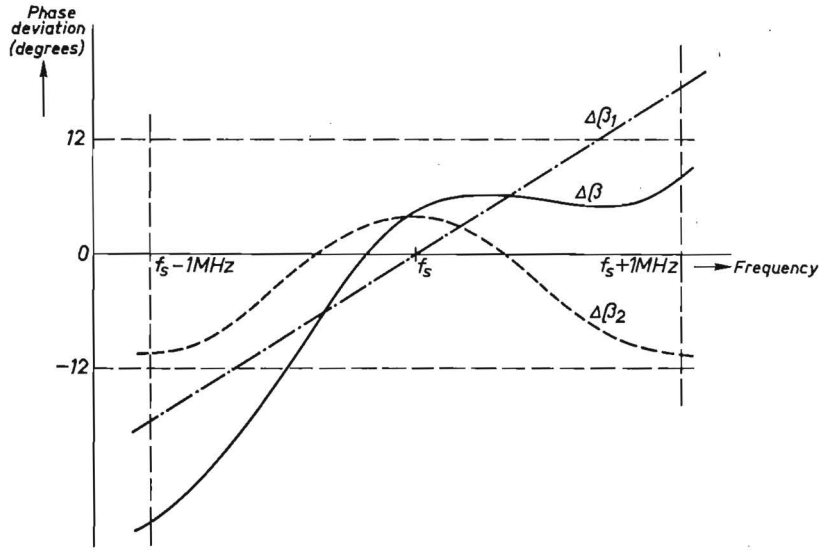


Fig. 2.5. Example of delay-line-phase response meeting the requirements.
$\Delta\beta_1$ = odd component, $\Delta\beta_2$ = even component,
$\Delta\beta$ = total deviation, f_s = colour-subcarrier frequency.

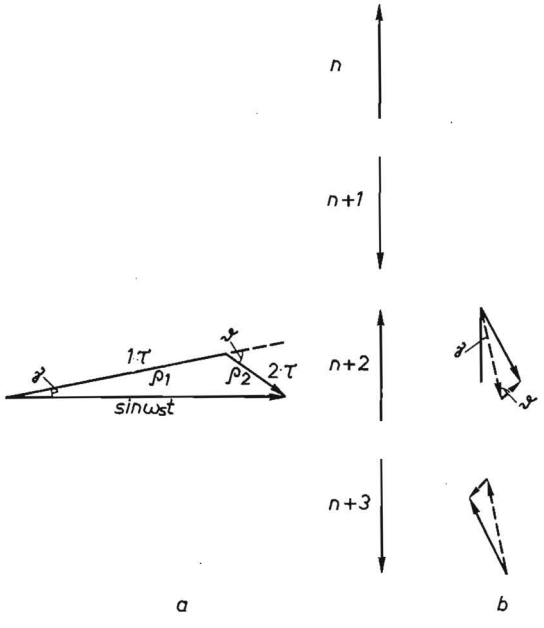


Fig. 2.6. PAL decoding process resulting from the employment of a delay line having 2τ reflections.

number times 2π) between the 1τ and 2τ output components. This angle ϑ, then, is a property of the delay line and its terminations, while γ is the result of the adjustment. According to our assumption γ is evidently adjusted so that

$$\varrho_1 \sin \gamma = \varrho_2 \sin (\vartheta - \gamma).$$

Figure 2.6*b* depicts the decoding process for a colour having no $(B' - Y')$ component. The input signal is shown in the first column, which shows the signal for four lines. The second column represents the signals delayed by the delay line, which is adjusted in the manner discussed above; the delayed signal of the third line consists of contributions by the undelayed signals of the two previous lines.

It may be concluded from an examination of fig. 2.6*b* that summation and subsequent demodulation in the horizontal direction, of the signals in the third row results in the signal

$$\text{detected sum} = \varrho_1 \sin \gamma + \varrho_2 \sin (\vartheta - \gamma) = 2\varrho_2 \sin (\vartheta - \gamma)$$

instead of resulting in zero. Furthermore, during the next line this demodulated-summation output will change polarity; thus the presence of 2τ reflections will result in Hannover-Bar-type errors.

We have tacitly assumed that the 2τ reflections did not appear over the input terminals. The assumption is justified if the undelayed signal is actually derived from a low-impedance generator or from a current generator, as is recommended for the type-DL1 line, to be discussed in the next chapter.

It is possible to adjust the delay line so that the $(R' - Y')$ colours are reproduced correctly; in this case, however, the Hannover-Bar-type errorre appears in the $(B' - Y')$ colours. In this respect 2τ reflections are seen to be more troublesome than 3τ reflections which, after proper adjustment, are not visible in large-area colours.

Tolerance in amplitude-frequency characteristic

We shall assume the ideal amplitude-frequency characteristic to give a response of unit amplitude within the chrominance bandwidth. Let the actual amplitude curve then be described by $\{1 - \varepsilon(p)\}$ where p is, as before, the modulation frequency. We need not say much about the tolerance at the subcarrier frequency. This error will only give a saturation error $(1 - \varepsilon/2)$. By means of the variable attenuator in the undelayed path of the decoder, this error can easily be made negligibly small. Of course the reproducibility of the delay-line-manufacturing process in this respect must be required to be good enough so that the attenuator does not need too large a correction range. An amplitude tolerance of a few dB is certainly acceptable. Actually it may be said that reproducibility is the manufacturer's main concern since, as experience has shown, poor reproducibility will make itself felt even more in some of the other

delay-line characteristics.

Assuming now a red-difference input signal $\pm S_{1m} \cos pt \cos \omega_s t$ and introducing

$$2\varepsilon_1 = \{\varepsilon(p) - \varepsilon(-p)\}, \tag{2.55}$$

$$2\varepsilon_2 = \{\varepsilon(p) + \varepsilon(-p)\}, \tag{2.56}$$

we find for the detected output signals:

$$\text{red-colour-difference-channel output} = S_{1m}(1 - \varepsilon_1/2) \cos pt, \tag{2.57}$$

$$\text{blue-colour-difference-channel output} = 0 \tag{2.58}$$

for the case

$$\varepsilon(p) = \varepsilon(-p), \tag{2.59}$$

and

$$\text{red-colour-difference-channel output} = S_{1m} \cos pt, \tag{2.60}$$

$$\text{blue-colour-difference-channel output} = \pm (\varepsilon_1/2) S_{1m} \sin pt \tag{2.61}$$

for the case

$$\varepsilon(p) = -\varepsilon(-p). \tag{2.62}$$

Evidently the roles of odd and even parts of the amplitude curve are more or less the reverse of those of the corresponding parts of the phase curve, as regards the effects which they produce.

Considering first the even part of the amplitude curve, it is seen to give a desaturation factor $(1 - \varepsilon_2/2)$. Here again precise experimental evidence as to the error which may be allowed in the sidebands is lacking. The experience acquired so far seems to indicate that it will be tolerable if the amplitude drops to 70% at the sideband frequencies of plus and minus 1 MHz. This would desaturate the 1-MHz chrominance components to 85% of the original value, which seems indeed very reasonable. Upon examination of eqs (2.40) to (2.43) it is found that the amount of desaturation caused by phase deviation is much smaller still, so that the full available desaturation tolerance may be reserved for the even-amplitude error.

The odd part of the amplitude curve is seen to cause an alternating hue error which is equivalent to a rotation in the S_1,S_2 diagram of $\pm \arctan(\varepsilon_1/2)$. Experience shows that it is possible to make the delay-line-amplitude characteristic fairly symmetric; thus it seems reasonable to require that the hue errors, caused by amplitude asymmetry, shall be at least a factor of 2 smaller than those caused by the even part of the phase curve. This leads us to require that the odd component of the amplitude shall deviate no more than $\pm$ 5% from the amplitude at the subcarrier frequency. In addition to these tolerances an ampli-

tude ripple due to reflections may be allowed. The *p-p* value of the ripple caused by 3τ reflections should be no more than 10%.

Further requirements

Obviously it is desirable to make the insertion loss as small as possible. This calls first for efficient conversion of electrical into ultrasonic energy and vice versa, and second for efficient gathering of the propagated sound beam on the output side. The delay-line design must lend itself to mass production. The necessity for a reproducible manufacturing process can hardly be overstressed.

All the tolerances on the electrical characteristics which were found or estimated in the previous pages should not be exceeded within the working range of temperatures; this range will be from 20° to 50 °C approximately. In addition the delay line should also operate reasonably well outside this range,

TABLE 2-I

PAL-delay-line requirements and tolerances

phase response at the subcarrier frequency $\beta_s = (m.180 \pm 12)°$ (m is an integer)	
chrominance bandwidth 3·4-5·4 MHz	
phase-frequency characteristic β $\beta = \beta_0 + \Delta\beta_1 + \Delta\beta_2$ with $\frac{d\beta_0}{d\omega} = 64\ \mu s$	
tolerance on odd part of phase deviation $d/d\omega\,(\Delta\beta_1 < \pm 50\,ns)$	within chrominance bandwidth
tolerance on even part of phase deviation $\Delta\beta_2 < \pm 12°$	within chrominance bandwidth
amplitude-frequency characteristic A; $A = A_0(1 - \varepsilon_1 - \varepsilon_2)$	
tolerance on odd part of amplitude deviation $\varepsilon_1 < \pm 0{\cdot}05$	within chrominance bandwidth
tolerance on even part of amplitude deviation $\varepsilon_2 < \pm 0{\cdot}3$	within chrominance bandwidth
reflections: 3τ reflection < 26 dB below main output other reflections < 30 dB below main output	
working temperature range 20-50 °C	

say to —20 °C on the one hand and to 70 °C on the other hand; these extreme temperatures must not be destructive for any of the line properties.

Stability of properties must also be required with respect to ageing. The input and output impedances should preferably be of the order of a few hundred ohms for transistor operation. Suppression of direct electrical break-through between input and output should be 35 dB or better. Finally, the delay line, since it will be a home-receiver component, must be quite inexpensive.

Summary

In table 2-I the main requirements and tolerances are grouped together. It should be emphasized that the information in this table cannot be very precise. In particular, the tolerances on the frequency characteristics are of a speculative nature. If the chrominance input signal in future receivers is reasonably undistorted, these tolerances may very well be too severe. Thus, it has been our purpose to estimate the electrical tolerances as well as possible and to analyze the relative importance of various characteristics. The tolerance for β_s is not so uncertain and the value given in the table should not be exceeded; it would in the author's opinion be worth while to stay well within that limit.

REFERENCES

2–1) W. Bruch, Nachrichtentechnische Zeitschrift **17**, 109-121, 1964.
2–2) W. Bruch, Telefunken-Z. **36**, 70-88, 1963.
2–3) F. W. de Vrijer, Philips tech. Rev. **27**, 33-45, 1966.
2–4) J. Davidse, Philips Res. Repts **19**, 112-280, 1964.

3. DISCUSSION ON THE PAL DELAY LINE TYPE DL1 AND ON ALTERNATIVE DESIGNS

3.1. Introduction

In this chapter we discuss the properties of the delay line, which was developed for use in domestic PAL receivers and which received the code number DL1. In addition, the relative merits of alternative designs will be discussed. The DL1 is an ultrasonic type of delay line; it can be characterized as a shear-wave folded-space delay line with ceramic piezoelectric transducers, having an offset angle for maximum suppression of the third-time-round signal.

In sec. 3.2 we investigate the suitability of non-ultrasonic lines. There follows, in sec. 3.3, a brief historic outline of ultrasonic delay lines. A general description of the DL1 is given in sec. 3.4.

Section 3.5 discusses the relative advantages and disadvantages of alternative delay-line designs. The chapter is concluded with a more detailed discussion on the properties of the DL1 line.

3.2. Non-ultrasonic delay lines

Under the heading of non-ultrasonic delay lines we briefly consider a few types; these fall into two categories, which we shall call first, electromagnetic delay lines, and second, electronic delay lines.

The simplest electromagnetic line is probably the video coaxial cable. The employment of such a cable for our purpose is entirely impractical due to the very great length needed to obtain 64 microseconds delay: the exact length would depend somewhat on the type, but more than 10 kilometres would in any case be required.

Cables having an outer conductor consisting of a coil fare better in this respect because the self-inductance per unit of length is greater: such cables are used in colour receivers to equalize the relative delays of the chrominance signals and the luminance signal. The delay needed in that case is a fraction of a microsecond, which is produced by a few decimetres of this type of cable. For our purpose many metres would be required, so that again their length alone would preclude their use.

The lumped-element delay line produces the same delay in a somewhat smaller space [3-1,2,3,4]). These lines are low-pass structures consisting of a number of sections containing self-inductances and capacities. The sections may or may not be identical and there may be mutual coupling between sections. Loosely speaking, the number of sections needed is proportional to the product of bandwidth and overall delay, the constant of proportionality depending on the particular type of structure. An illustrative example is afforded by the line, discussed by Turner [3-2]), consisting of T and bridged-T sections in alternating

succession. Turner's calculations result in a delay-per-section of approximately 80 nanoseconds for a line which is to have a reasonably constant delay over a bandwidth of 5 MHz. Thus 800 sections would be required to give a delay of 64 μs. Made with conventional components the volume of this line would be several orders of magnitude greater than even the most generously dimensioned ultrasonic delay line. Volume and complexity are therefore the main disadvantages of the lumped-element line.

Recently a different kind of delay line has been developed and reported in the literature. This is an electronic type of delay line, referred to by Hannan et al. [3–5]) as a "bucket-brigade" delay line. In this line, a signal is represented by a charge on a capacitor; there is a cascade of at least as many capacitors as there are signal values to be stored. By transferring the charge from one capacitor to the next in line, the signal "propagates" through the structure. Transference takes place by means of electronic switches which operate at rates determined by driving signals. The propagation speed and thus the overall delay time may be chosen simply by choosing the frequency of the driving signals. From the foregoing description it follows that again the number of elements needed (consisting of capacitors and active elements) is proportional to the highest signal frequency and the delay time. Choosing three as a safe constant of proportionality we find that approximately 900 of such elements are needed. This line, with the necessary associated circuitry, is even more complicated than the lumped-element line and only a few years ago such lines could have been considered only for extremely small storage capacities. A circuit such as the bucket-brigade line, consisting as it does of a great many identical stages, lends itself very well to integration techniques, so that in applications where the feature of the electronically variable delay time is needed, this line may well provide a solution. For our purpose, however, this feature would constitute a disadvantage, since a high degree of constancy in the delay time is needed. In any case, it would seem that much development work in integration techniques will have to be done before a circuit of this kind can compete in price with a structure as simple as that of the ultrasonic delay line.

3.3. Historic survey

The propagation speed of acoustical waves in most solids is of the order of several kilometres per second, approximately one hundred thousand times smaller than the velocity of electromagnetic waves in coaxial cables. Ultrasonic delay lines are therefore very suitable for producing delays of more than about one microsecond, the limit beyond which the lines discussed in the previous section tend to become voluminous and complicated.

The general construction of an ultrasonic delay line is simple enough: it consists of an input transducer which converts the electrical signal into mechanical vibrations, a propagation medium and an output transducer which recon-

verts the mechanical energy into electrical energy. On occasion one transducer may be omitted, the remaining one functioning as both input and output transducer. Yet within this simple scheme many variations are possible, and the amount of literature dealing with the subject is correspondingly large. General surveys on types and applications of delay lines have been given by Palfreeman [3-6]), Arenberg [3-7]) and Eveleth [3-8]) to name but a few. A survey of the application of ultrasonics, of which ultrasonic delay lines form a branch, is presented in an article by Mason [3-9]). A book by Brockelsby, Palfreeman and Gibson [3-10]) discusses systematically various classes of delay lines, giving the underlying theory, examples of construction and applications. Volume 1, Part A of a series of books on Physical Acoustics, edited by Mason [3-11]) contains chapters on guided-wave lines and on multiple-reflection lines.

Ultrasonic delay lines and ultrasonic techniques in general have found many applications in military as well as in civilian fields. The ground work for the realization of ultrasonic delay lines was laid in 1880 when P. and J. Curie discovered the phenomenon of piezoelectricity [3-12]). Their discovery of the reverse effect in the same quartz crystals soon (1881) followed. Large-scale applications of this discovery were not immediately forthcoming, nor were the first applications in the field of delay lines. During World War I Langevin developed transducers for the detection of submarines and underwater obstacles [3-13,14]). In the period between the two wars a significant commercial use of ultrasonics was the application of quartz-crystal vibrators in channel filters for broadband telephony [3-15]). The development of delay lines was greatly stimulated during World War II when radar techniques required the employment of accurate delay lines, having large delay times and large bandwidths. In the United Kingdom this work was concentrated at the TRE, and in the United States of America at the MIT. The first delay lines developed in those countries for radar purposes were liquid lines [3-16,17]). Solid propagation media were, to a lesser extent, also investigated but the main effort was directed towards the liquid line. This was largely due perhaps to the fact that more experience was available on liquid lines; other disadvantages of solid lines, mentioned at that time, were the propagation-mode conversion and the attenuation in solid media. It should be mentioned that delay times of the order of milliseconds were required for Moving Target Indicator Radar equipment, so that attenuation was an important feature. An advantage of the liquid line was the ease with which the delay time could be varied. The first glass delay line was developed during the same period in Germany. As follows from the original patent [3-18]), this glass line served radar purposes also; it is generally known under the name of "German range marker glass line".

Much research and development in transducer materials has been done since the early 'forties. Up to that time quartz was the most important material, but there were also smaller fields of application for rochelle salt and tourmaline.

Synthetic ammonium dihydrogen phosphate (ADP) crystals were added to this range of useful materials during World War II when they were used in large transmitting and receiving arrays for the detection and location of submarines [3–19]. Mason reported in 1947 [3–20] on the suitability of crystals of ethylene diamine tartrate (EDT) for use in telephone plants. In about 1947 there was increased interest in the piezoelectric properties of barium-titanate ceramics; see for example an article by Roberts [3–21] (1947). It was found that the ceramics could have high electromechanical coupling factors and it was discovered also [3–21,22,23] that the piezoelectric effect is remanent to a large extent. This material owes its high electromechanical activity to ferroelectricity. Ferroelectricity (spontaneous polarization) had been discovered long before in the afore-mentioned rochelle salt; the effect was first often termed seignette electrics. The properties of rochelle salt are otherwise very different from those of the ceramics. The salt exhibits spontaneous polarization only in the temperature range of —18 °C to 24 °C. Outside this range the material is nevertheless piezoelectric to an important degree. Due to its temperature dependence and to its complex dependence on humidity, rochelle salt has a limited usefulness. Barium-titanate ceramics are ferroelectric below the Curie temperature of 116 °C. Some of the advantages of the new material are: first, it is not necessary to make accurate cuts in certain given directions, so that there is no need to X-ray the material; and second, more complex transducer shapes can easily be made. Disadvantages are that poling needs to be performed at some appropriate stage during manufacture and that subsequent operations (such as polishing and bonding) should be done at temperatures far below the Curie temperature. In 1951 Shirane and Hoshino [3–24] reported on the very high spontaneous polarization which they expected to be present in their lead-titanate ceramics; in 1954 and 1955 Jaffe, Roth and Marzullo [3–25,26] described the piezoelectric properties of lead-zirconate-titanate solid-solution ceramics. A few years later a wide choice of such ceramics was available, several of these lead-zirconate-titanate ceramics having Curie temperatures as high as between 300 and 400 °C. Fortunately such materials were available at the time the present investigation into the PAL-delay-line problem started.

As regards the applications of ultrasonic delay lines, we find that they are not nearly as numerous as applications of ultrasonic techniques in general. Apart from their use in radar and, later, computer equipment, we may mention that ultrasonic delay lines have found their way into the television field also.

The earliest example is the line used in the Scophony receiver [3–27], which has however not come into general use. A recent application is the vertical-aperture-correction delay line which is being used to increase the vertical resolution of television cameras; other examples have been discussed by Brockelsby and Palfreeman [3–27].

A common factor in the applications mentioned is that they are in the

professional field; the PAL and the SECAM delay line are the first delay lines which will be components in consumer products. This fact has, of course, had some bearing on the choice that had to be made regarding the type of delay line to be used in PAL receivers.

3.4. Description of the PAL delay line

In this section we describe the chosen design for a PAL delay line. Figure 3.1 shows two projections of the line. T_1 and T_2 represent respectively the input and the output transducer. The propagation body G is made of a glass specially developed for the purpose. The propagation of the mechanical waves is in the direction of the arrows. As the figure shows, use is made of one reflection facet. Propagation is by shear waves with particle movement parallel to the reflection facet.

The two transducers are identical and fig. 3.2 shows one of them in more detail. The non-shaded part in this figure represents the transducer material, the shaded areas are the electrodes. The transducer dimensions are $10 \times 12 \times 0{\cdot}23$ mm^3 approximately and the transducer material is Piezoxide 3 or PXE 3 *). PXE 3 is a solid solution of lead zirconate-titanate [3–24,25,26]; it has a relatively high Curie temperature (395 °C) and a high electromechanical coupling factor for thickness-shear vibrations (between 0·6 and 0·7 after the usual manufacturing steps). Before the deposition of the electrodes, the material is polarized

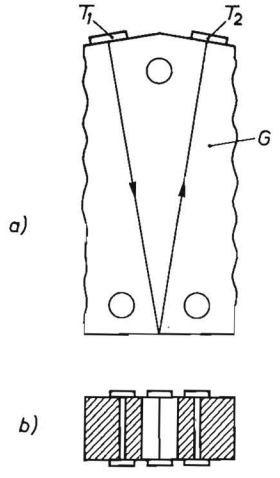


Fig. 3.1. PAL delay line. (*a*) T_1,T_2: transducers, G: glass propagation body. (*b*) In this view the transducers are omitted; the shaded areas represent electrode layers.

*) Piezoxide and PXE are trademarks of N.V. Philips' Gloeilampenfabrieken Eindhoven; see also the bulletin "Piezoxide" edited by the Philips Industrial Components and Materials Division, May 1963.

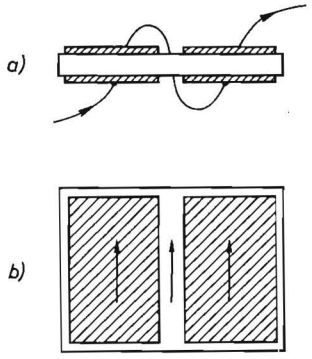


Fig. 3.2. Transducer. View (*a*) shows schematically the connection of the electrodes; shaded areas represent electrodes; the arrows indicate the direction of polarization.

in the direction shown by the arrows in fig. 3.2 and care is taken to make the polarization as homogeneous as possible.

The electrodes are thin metallic layers, deposited upon the piezoelectric material by the process of vacuum evaporation. Each layer consists of two layers. An inner layer of nickel-chromium and an outer layer of nickel. The materials for these layers have been chosen so that the inner layer gives good adherence to the substrate while the outer layer produces a surface on which it is easily possible to solder. The thickness of the two layers combined does not exceed 0·5 μm. Each electrode is divided into two parts and the parts are connected by wires as shown schematically in fig. 3.2. As all the transducer impedances are inversely proportional to the radiating area, the electrical impedance of the transducer shown is equal to that of two transducers connected in series, each having twice the impedance which an undivided transducer would have. The resulting impedance gain of 4 was considered desirable since the impedance of the undivided transducers at the frequencies considered and for this rather large radiating area would be very low, due to the high dielectric constant of the ceramic material. The electrical connections as shown in fig. 3.2 are made so that the applied electric field has the same direction in both regions of one transducer. Thus, the mechanical behaviour of these transducers is influenced very little by this technique, provided that the dividing lines are made narrow.

The glass body has roughly the shape of a parallelepiped having its top facet replaced by the two transducer facets shown. The overall dimensions are approximately $80 \times 40 \times 18$ mm^3. The transducer facets and the reflection facet are flat; the two major and the two minor faces (the "walls" of the propagation body) show ripples. These ripples may be clearly seen in the picture of fig. 3.3; for the sake of clarity they were omitted in the lower projection of fig. 3.1. They serve to scatter the radiation which reaches the walls and thus to diminish the influence of the various kinds of reflections. Protruding from the major faces

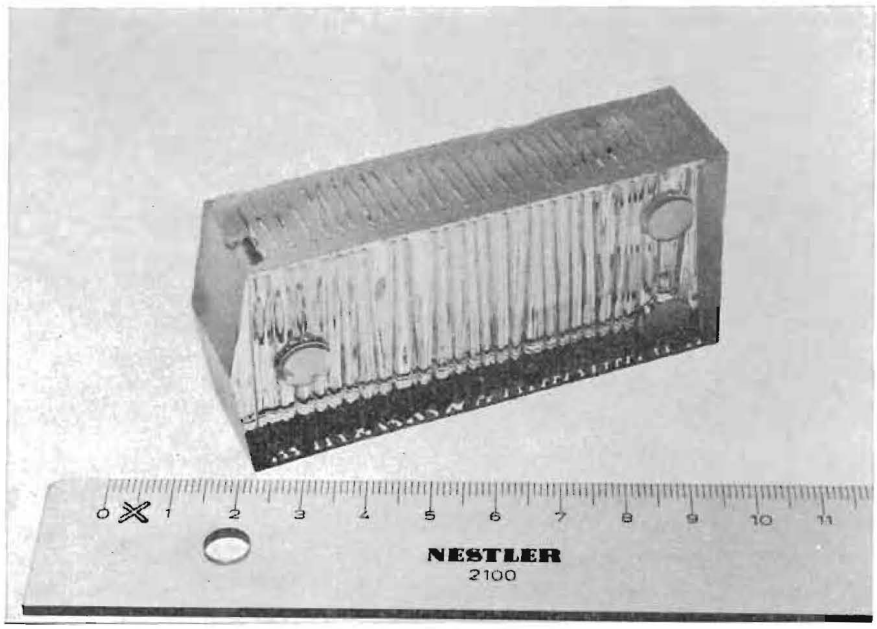


Fig. 3.3. Glass propagation body.

are six studs, the function of which will be explained below.

By far the most stringent requirement which the glass had to satisfy was the very low variation of time delay as a function of temperature. For the PAL line the relative variation should not exceed approximately $\pm$ 1 in 20 000 within the operating range of temperatures. The glass was developed for this purpose by the Philips Glass Development Centre; it is a potash-lead-silicate glass. The time-delay variation caused by the propagation body is of course determined by the variations in the dimensions as well as by the variations in the propagation speed of the mode used. If these two contributions are balanced by careful selection of the composition and the heat treatment of the glass, an isopaustic glass is obtained. Actually the Glass Development Centre has gone one step further; they have included the temperature-dependent delay contribution of the transducers amongst the variations to be canceled out [3–28]). For more detailed information on the glass, which has been given the code number 239, the reader is referred to an article by Zijlstra and Van der Burgt [3–29]); this article also contains a number of references on the subject.

The shear-wave velocity of the glass may vary somewhat from batch to batch. If all lines were made with the same dimensions, therefore, they would still show a spread in delay time. Early practice, with a different type of delay line [3–30,31]) has been to make the delay time a little too short (including the spread) and to add a delay obtained from a short variable electronic delay line. If it is desired,

however, to obtain the correct delay without the additional variable line, it becomes necessary to adjust the path length in the ultrasonic delay line. With a delay medium having at least one reflection face, such as the type described here, the adjustment can very accurately be carried out since one has the possibility of grinding the reflection facet while electrically monitoring the delay. This final delay adjustment must be put off until the stage when the transducers have been mounted and wired in. Since the transducer faces need to be ground also, it follows that there must be two different stages of grinding. And since the glass body must be held in identical positions during these two grinding stages, it must be provided with ground reference planes. The three ground studs on one of the major faces constitute one reference plane. Advantages of using the studs are: first, there is less glass to be ground and second, there is no chance of grinding away the ripples [3-32]). It has proved to be not very difficult to obtain, in the laboratory, a phase-delay accuracy of better than one nanosecond; on a mass-production basis, an accuracy of a few nanoseconds is maintained. Further details on the adjustment process are given in the chapter on measurement methods; this chapter also gives the main characteristics of the delay line. These characteristics are generally valid if coils of specified value are connected parallel with the transducers and if the specified generator and load impedances are employed. For the DL1 (the code number of the delay line here described) these impedances are resistive and each 150 Ω. The coils are considered as part of the DL1.

A photograph of the finished delay line is shown in fig. 3.4.

3.5. Alternative designs

In this section we will examine the relative merits of alternative PAL delay-line designs. This will be done by successively finding what limitations are imposed by the PAL requirements regarding such properties as delay variation with temperature, phase accuracy, and so on. Advantages of this procedure are: first, it provides a logical approach and second, by the process of elimination it becomes unnecessary to discuss all the conceivable designs. Some designs can be discarded simply because they do not fulfil one or more PAL requirements. There are other designs which are acceptable on purely theoretical grounds but which cannot be produced inexpensively. In such cases it is really the state of the art which is being discussed.

3.5.1. *Attenuation, bandwidth*

The characteristics of attenuation and bandwidth are considered together since to some extent we can improve one of them at the cost of the other. The requirements as far as attenuation and bandwidth are concerned are not, by today's standards, extremely high and therefore do not rule out many delay-line materials or geometries. They do eliminate the use of piezoelectric trans-

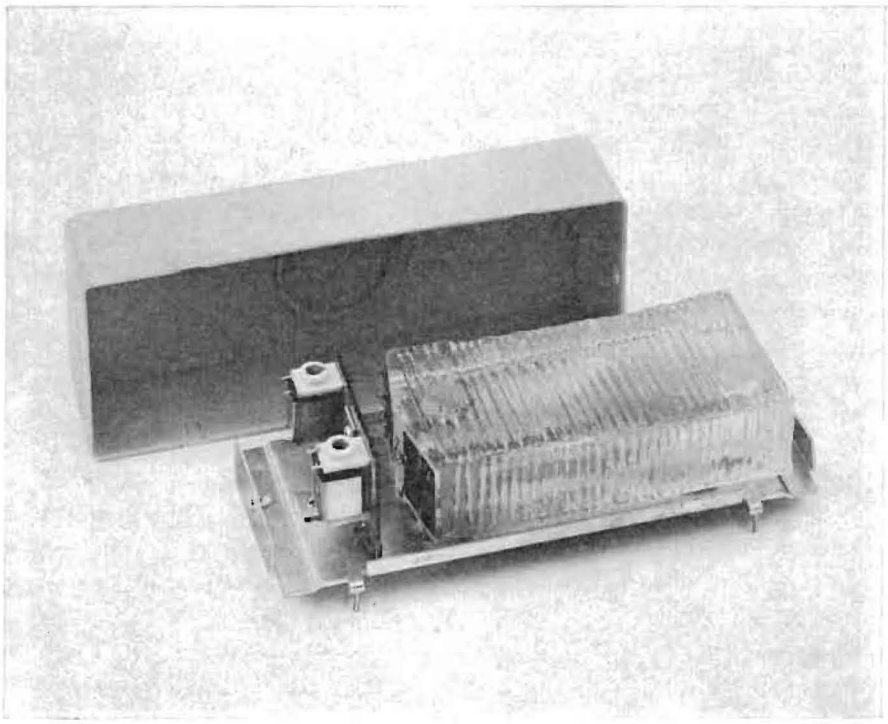


Fig. 3.4. Finished delay line; cover removed.

ducer materials with electromechanical coupling factors as low as those of quartz, since lead-zirconate-titanate ceramics have much higher coupling factors while their other properties are quite acceptable for the purpose.

Very unsuitable also are transducer coils used in conjunction with magnetostrictive wires or tapes, as used in the wire delay line operating with extension waves and in the Scarrott-and-Naylor type of wire line with torsional waves.

If piezoelectric transducers, operating either in the thickness-shear or in the thickness-expander modes, are employed, then we require a reasonable match between the mechanical impedance of the propagation material and the appropriate mechanical impedance of the transducer. Here we have disregarded the possibilities which there may be in the use of a bonding layer of finite thickness between transducer and propagation material; such techniques of course tend to increase the cost price. We shall examine the influence of matching in more detail when we deal with reflections and also in the chapter on transducers. It will turn out that this requirement is not very critical, as long as the transducer coupling factor k for the vibration employed is as high as approximately 0·6. Such coupling factors are easily obtainable with lead-zirconate-titanate transducers.

3.5.2. *Delay variation with temperature*

The very high temperature-stability requirement at for the PAL delay line leaves very little choice in the materials to be used for the propagation medium. The use of an oven with temperature stabilization was considered undesirable since it would make the delay line more expensive and the receiver would be operative only after a certain warm-up time. As far as the author knows, a few years ago, when the investigations on this subject were started, there were only two classes of materials that showed promise as regards their time-delay stability: lead-potash-silicate glasses on the one hand, a few nickel alloys on the other hand. At the time of writing this situation is essentially unchanged. Of the nickel alloys, a material known as Ni-Span C *)[3-33] is a good candidate; a similar material is Thermelast **). These alloys, however, were and are very expensive, and to keep the price down to a reasonable level it would be necessary to choose strip or wire lines. Thus, we may be very brief on this point; the temperature-stability requirement dictates the use either of certain glasses or of certain nickel alloys. In the latter case a guided-propagation shape, such as strip or wire, seems indicated.

3.5.3. *Phase-delay accuracy*

As we have discussed before, the desired tolerance on the phase-delay time is approximately $\pm$ 3 nanoseconds. An adjustment of the phase delay of a delay line may be effected by "detuning" the delay line, that is, by changing the value of the reactive component of load and/or generator impedance. The range of this adjustment, however, should be kept very small — $\pm$ 5 nanoseconds —, since detuning influences several other characteristics besides the phase delay. For example the level of the reflections is sensitive to changes in the terminating impedances. It is preferable therefore to satisfy the phase-delay requirement by adjusting the length of the propagation path.

It is convenient to divide delay lines into two categories: those whose propagation length can easily be varied and those whose length cannot easily be adjusted. By variable-length lines we mean delay devices whose transducers are not fixed to the propagation medium; an example is the well-known video wire delay line [3-34,35]) operating with transducer coils which can be moved along the wire. We do not expect the bullk properties of technical glass or nickel alloys to be so constant from batch to batch that a constant propagation medium path length will always result in a phase delay which is constant to a few nanoseconds. For example, experience with glass lines has shown that the phase-delay time for lead-alkali-silicate-glass lines may show a spread of two per cent if the dimen-

*) Ni-Span C is a registered trademark of the International Nickel Company.
**) Thermelast is a registered trademark of the Vacuum Schmelze A.G.

sions are held constant. At first sight, then, it might seem attractive to choose for a PAL delay line one of the variable types. Examples are (a) the video wire line [3-34,35]) often called the magnetorestrictive delay line, which operates with extensional propagation modes; (b) the Scarrott-and-Naylor [3-36]) type of line, in which again extension waves are generated and detected, but where mode converters ensure that the main delay is caused by the propagation of torsion waves in a wire; (c) the delay line with Wiedemann [3-37]) transducers producing torsion waves in a wire by making use of the Wiedemann effect. All three types operate with transducers coils, which may be mounted on lead screws. In the previous section we have all but ruled out the use of coils, so we will not examine in detail the designs employing such transducers. In any case the idea of employing a variable-length line loses much of its attraction upon closer examination. As the propagation velocity will be of the order of 3 km/s a path adjustment of 3 μm is needed. Lead screws would not allow sufficiently accurate adjustment. A more elaborate and very rigid arrangement would probably be required. In addition the dimensions of the housing would co-determine the delay time and thus this housing would have to be rigid as well. The thermal properties of the housing would enter into the temperature dependence of the delay time. We conclude that the feature of variability would, for the PAL application, be a distinct disadvantage.

It is preferable then to employ lines with fixed transducers. In the author's opinion it is highly desirable that an additional variable electronic delay line should not be needed; we assume here that the required phase-delay accuracy will have to be produced by the acoustic delay line without additional correction. We have found that this assumption leads us to require that there should be a reflection in the propagation path, i.e. "folded acoustics" should be employed. The object, of course, is to have available a free reflection face so that the delay can be adjusted by grinding away this reflection facet. The need for this kind of adjustment was brought out quite clearly when we carried out experiments to determine the feasibility of adjusting the delay time of a simple bar type of space-delay line. This line consisted of a glass bar having a transducer at each end. Adjustment had to be performed as follows. First the delay of a finished line was measured; then one transducer was removed and a calculated length of glass was ground away; finally the missing transducer was remounted. For the production of delay lines with the required delay accuracy we found this procedure entirely impractical; it would be an uneconomic approach even for the production of a small series.

We conclude that delay lines with fixed transducers and folded acoustics are needed. This rules out all wire-type lines unless we accept lines employing but one transducer. In such a wire line one would still have a free reflection face. Bruch [3-38]) discusses two ways of making the one transducer function both as transmitter and receiver. A circuit for using mono-transducer lines useful in a

SECAM receiver has been described in a patent application [3-39]).

It may well be possible to employ folded acoustics in a strip line. The device called width-shear delay line by Eveleth [3-8]) is such a line. The author has not yet found, however, a thorough theoretical and practical discussion on a folded-acoustics strip line. Meitzler [3-40,41]) gives a theoretical treatment and reports practical results of strip delay lines, but these are not folded types.

Much more [3-8,10]) is known on the subject of folded-acoustics space lines, the word "space" indicating that the dimensions perpendicular to the propagation path are large with respect to the wavelength. This type of geometry is very suitable for our purpose. The number of possible shapes is large. Besides the "Vee line" (one reflection), there are multiple-reflection lines such as various wedge lines, billiard-table lines, polygon lines and so forth. An advantage of employing multiple-reflection lines is that their volume is smaller. But adding reflections increases the cost price since the angular-accuracy requirement becomes more severe; in addition it becomes more difficult to keep the spurious signals below an acceptable level. If one reflection facet is used for two reflections — separated by an odd number of reflections at other faces — then the line becomes, to some extent, indifferent to angle errors of this particular facet and therefore it is an advantage to use such a facet for the adjustment by grinding. Again this advantage should not be overrated: although the angle accuracy in one plane is relaxed, this is not the case for the angle in a plane perpendicular to it. A detailed discussion on multiple-reflection lines is given under the heading of "Solid Lines" by Brockelsby et al. [3-10]) who also mention the advantages of using shear waves.

3.5.4. *Dispersion*

As follows from the discussion on PAL-delay-line requirements, very little dispersion is allowable, and so a non-dispersive type of delay line should be selected. The term non-dispersive usually applies to the mechanical wave-propagation properties of the line. Of course, the dispersion is not solely determined by the propagation properties; another part is contributed by the transducer pair. We will discuss transducer characteristics in a separate chapter. There exists a large amount of literature on the subject of wave propagation alone. An extensive list of references is given in a review by Miklowitz [3-42]). Propagation in infinitely long cylindrical rods and in plates, also having infinite propagation lengths, and having relatively small, as well as finite transverse dimensions, have been fairly thoroughly investigated. Often a particular propagation mode is assumed and there ensues a relationship between phase velocity, frequency, the main dimension of the medium and its elastic properties applicable to this mode. The relationship is known as the frequency equation, or the transcendental frequency equation; each mode has its own equation. For a survey of this field the reader is referred to the chapter by Meeker and Meitzler

in Mason's work [3-11]), which gives a unified treatment of the subject, many phase-velocity–frequency curves and numerous references. A propagation mode, as the word suggests, describes the propagation along an infinitely-long-delay medium. Usually it is assumed that the difference between this description and the behaviour of a delay line of finite length may be disregarded.

Two well-known non-dispersive propagation modes are: the fundamental torsional mode in cylindrical rods or wires and the lowest symmetrical SH mode in the infinitely wide strip. Other modes may be made non-dispersive to as high a degree of approximation as the circumstances allow. Examples are the extensive waves in a wire, if the product of diameter and frequency is sufficiently small, and various possible ways of wave propagation in space-delay lines.

Although it has been made clear in the previous section that wire lines are not very suitable for our purpose, let us briefly investigate the limitations which the dispersion requirement imposes on wire lines. The description of the fundamental torsional-mode vibration has been given by a number of authors, see for example Love [3-43]), Kolsky [3-44]) or Mason [3-11]). For a given upper frequency to be propagated there exists a wire or rod diameter which should not be exceeded if it is desired that only the fundamental mode be propagative. The reason for wanting only the fundamental mode is that the higher modes are dispersive. The critical diameter d follows from

$$d = \frac{2\,V_s}{\omega_m}\,5{\cdot}136,$$

where V_s is the bulk-shear velocity and ω_m the maximum angular frequency which the line is required to handle. Substituting for V_s the value 3 km/s (the wire is assumed to be made of an alloy such as Ni-Span C) and $2\pi\,5{\cdot}4.10^6$ for ω_m, we find that the wire diameter should not exceed 0·9 mm. This would be a convenient value as regards the handling of the wire itself; but as regards the fabrication, handling and mounting of the various possible transducers, it seems an inconveniently low value. We mention three of these possible transducers: the Scarrott-Naylor transducer [3-36]), the Wiedemann [3-37]) transducer and a two-piece transducer described by Thurston and Anreatch [3-45]). We have already discussed some of the disadvantages of the first two types. We may add that the Scarrott-Naylor transducer would constitute a rather complex structure and that, at these high frequencies, it would be very difficult to get a reasonable match between the extensional and the torsional elements. As to the Wiedemann line, its insertion loss would be very high indeed; also it would have the drawback of the large current which would have to be supplied through the propagation wire. Perhaps the only acceptable torsion-mode transducer would be the two-piece transducer described by Thurston and Anreatch [3-45]). This device has the attractive feature of being homogeneously polarized and excited, so that one may expect the effective electromechanical coupling factor

to be good. It would be necessary to prevent the electric tension from being short-circuited by the wire.

We shall not dwell upon the wire line with extensive wave propagation. A calculation would show that its diameter would have to be much smaller than that of the torsion wire line.

The other well-known example of a non-dispersive propagation mode is the lowest symmetrical SH mode in the infinitely wide strip [3-40,41]). The thickness of the strip needs to be kept below a critical value in order to prevent higher modes (which are again dispersive) from being propagative. The relation for the case is given by

$$t = \frac{\pi V_s}{\omega_m}.$$

Substitution of the same values as above leads to a critical thickness of 0·28 mm, or approximately three times smaller than the required wire diameter for the torsion line. The required SH waves may be generated in essentially the same way as are the shear waves in a space line. For example ceramic transducers with their polarization in the direction of the strip width and their electric excitation field in the propagation direction, may be employed. Two of the three dimensions of the transducer are now quite small, requiring careful study of the technique for handling the rather brittle transducers.

Space lines are not necessarily non-dispersive. For example, they may be dispersive if the lateral dimensions of the propagation medium are too small. It has become customary to speak of space lines whenever the lateral dimensions are larger than 10 to 20 times the wavelength employed. This criterion however does not ensure that the walls will exert no influence on the dispersion of the line. As the length of the line is increased and the cross-section of the transducer is made smaller (giving a less sharp radiation pattern) the sound energy reaching the walls will become a larger fraction of the total energy.

Even if lateral dimensions are infinite one still cannot conclude that the propagation is non-dispersive. For this to be the case additional geometrical conditions need to be imposed. They involve the use of either very small or very large transducers. Both types of conditions are impractical for the PAL delay line. However it does not follow that the space-line geometry is unsuitable for the PAL delay line as the propagation dispersion for realizable cases may be small. As an illustration, we calculate the dispersion of the DL1. Assuming the lateral dimensions of the propagation medium to be infinitely large, it can be shown that

$$W = \iint \frac{j}{\lambda} \frac{\exp(-jkr)}{r} \left(\frac{1 + \cos\theta}{2} \right) df_1 df_2, \tag{3.1}$$

where W is the displacement component integrated over the output area. We

take the following set of values:

transducer dimensions (input and output)	10×12 mm^2,
bulk-shear-wave velocity (glass 239)	$V = 2{\cdot}54.10^3$ m/s,
approximate nominal delay time	$T = 64$ μs,
length of line	$L = 160$ mm.

Numerical calculation of the integral of (3.1), in which we have substituted $\exp[-jk(R-L)]$ for $\exp(-jkR)$, gives the dispersion curve and the amplitude response of fig. 3.5. This substitution facilitates the computations by ensuring that the nominal group delay of 64 μs is subtracted from the end result; we have called the resulting phase and group delay, extra phase and extra group delay, resp. The calculated dispersion is very small indeed.

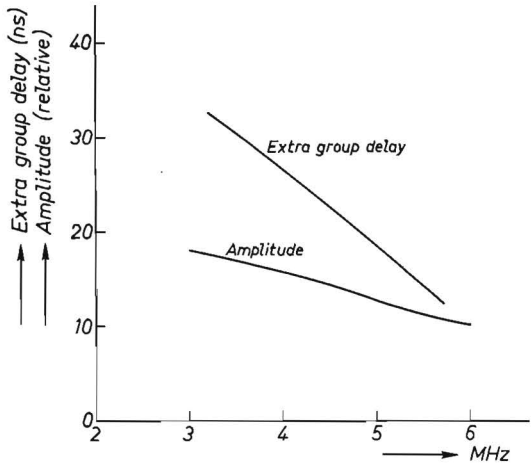


Fig. 3.5. Calculated group delay and amplitude response of delay line having unbonded cross-section. Shear-wave velocity in propagation medium (glass 239): 2·54 km/s, length of propagation medium: 160 mm, transducer radiating areas: 10×12 mm^2.

3.5.5. *Conclusion*

Of the many types of delay line we could make by combining various existing techniques, geometries and materials, few are suitable for the PAL application. We have demonstrated that the disadvantages of wire lines, particularly wire lines operating with transducer coils, are many. It is perhaps possible to construct a nickel-alloy-strip delay line with shear-wave propagation and one or more reflections in the propagation path; this conjecture is however not supported by theoretical or practical work. It may even be possible — if the technical difficulties can be surmounted — to fabricate such strips from thin potash-lead-silicate glass. A space type of delay line, made of this glass and provided with a folded propagation path, is very suitable for our purpose and it is the easiest to fabricate.

3.6. The PAL delay line: discussion and results of measurements

This section discusses in more detail the PAL delay line, type DL1, which was briefly described in an earlier section. Results of measurements of various properties are given.

3.6.1. *Attenuation, reflections, bandwidth*

Four types of losses may be seen to contribute to the overall attenuation; these are reflection, beam divergence, medium and miscellaneous losses. An example of the latter category is the loss resulting from an error in the angular position of a reflection facet or a transducer facet. This error may be accidental, such as might be caused by the spread in the manufacturing process. On the other hand, it may not be an error in the normal sense, but a desired deviation from the ideal angle, as exemplified by the offset angle employed for relative suppression of 3τ reflections at the subcarrier frequency.

It is of interest to know the relative contributions of these four categories to the overall attenuation; we will examine this distribution, in an approximate manner, for the DL1. Let us take the insertion loss (I.L.) — a definition of I.L. has been given by Thurston [3-46] — to be 8 dB. We assume the input signal to consist of r.f. pulses of chrominance frequency much shorter than 64 μs, yet long enough for their frequency composition to be reasonably sharp.

First we calculate the loss which the reflections caused by non-matched transducers, contribute. In fig. 3.6*a* the part between the terminals represents an unbacked transducer; all the mechanical quantities have been transformed into electrical quantities. The electrical port of the transducer is loaded by the resistance R_L and by the parallel tuning inductor L_p. On the mechanical side, the transducer is bonded to a medium represented by the resistance R_m; R_m is

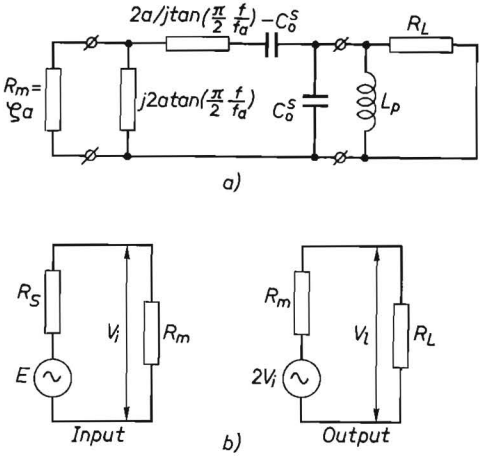


Fig. 3.6. Loss caused by reflections.

the mechanical impedance of the delay medium which again has been transformed into the corresponding electrical quantity. The bond thickness is negligible since it is only about 1/40th of the wavelength and so R_m may be connected directly across the mechanical port. This circuit is derived and discussed in the chapter on transducers. It will be shown there that

$$\zeta = \frac{\varrho_1 V_1}{\varrho_0 V_0{}^D},$$

where ϱ_1 and ϱ_0 are the densities of delay medium and transducer medium, respectively; V_1 and $V_0{}^D$ are the phase velocities of travelling shear waves in extended media: V_1 in the delay medium, $V_0{}^D$ in the transducer medium under the condition of constant electrical displacement. Thus ζ is the ratio of the specific mechanical impedances of delay material and transducer material. For the DL1 line we will find

$$\begin{aligned} \zeta &= 0{\cdot}45, \\ a &= 131{\cdot}2\ \Omega, \\ R_m &= 58{\cdot}8\ \Omega, \\ R_L &= 150\ \ \Omega. \end{aligned}$$

Here we have already multiplied the transformed mechanical impedances a and R_m by four, to take account of the fact that divided transducer electrodes are used. Tuning, by means of the adjustable inductor L_p, is effected approximately in such a manner that the parallel circuit formed by L_p and $C_0{}^S$ and the series circuit formed by $-C_0{}^S$ and $2a/\mathrm{j} \tan [(\pi/2) f/f_a]$ resonate at the same frequency. The series resonance frequency f_a' is given by

$$\tan x = \frac{x}{k_{15}{}^2},$$

where

$$x = \frac{\pi}{2} \frac{f_a'}{f_a}.$$

This can be deduced from fig. 2.6*a* if we add that

$$a = \frac{1}{8 k_{15}{}^2 f_a C_0{}^S}.$$

For $k_{15} = 0{\cdot}6$ we find that f_a' is about 15% lower than f_a. The design of the DL1 is such that f_a' is close to the chrominance frequency of 4·43 MHz. At the frequency f_a' the impedance $j\,2a \tan [(\pi/2) f/f_a]$ which is connected parallel to the mechanical port equals approximately $j8a$, a large value compared with R_L. Thus the transducer presents, to a good approximation, a resistance of R_L, or 150 Ω, to the mechanical waves arriving at the medium-transducer interface. The reflection factor ϱ therefore is given by

$$\varrho = \frac{R_L - R_m}{R_L + R_m} = 0{\cdot}44, \tag{3.2}$$

and the transmission t by

$$t = 1 + \varrho = \frac{2\,R_L}{R_L + R_m} = 1{\cdot}44. \tag{3.3}$$

Equation (3.3) leads to the equivalent circuit shown in the right part of fig. 3.6*b*, which holds for a receiving transducer receiving pulses of the midband frequency. Fig. 3.6*b* now represents the entire delay line. From this figure we deduce that, if

$$R_S = R_L,$$

which holds true in our case,

$$V_l = \frac{1 - \varrho^2}{2} E.$$

For the DL1 we have

$$V_l = 0{\cdot}404\,E.$$

A number of articles have been written on the subject of our second category of losses: the losses caused by beam divergence [3–47,48,49,50,51]). Although the articles cited include diffraction effects, they cannot be considered to give exact loss results since they generally assume (a) propagation in a fluid and (b) the absence of walls. The influence of both factors in our case is probably small enough to be acceptable for a rough estimate. Assuming, as a fair approximation of the actual DL1 line, the receiving and transmitting transducers to be disks with diameter of 13·2 mm, spaced 160 mm apart, a loss of 2·5 dB can be found from table I in an article by Seki, Granato and Truell [3–48]).

An offset angle of 45′ is employed in the DL1 delay line. The transducer dimensions are 10 by 12 mm and the normal to the transmitted-wave front makes respective angles of 90° and 90°45′ with the 10- and 12-mm sides of the receiving transducer. Inserting these values in the known directivity function for rectangular sources [3–10]) we find an amplitude loss for the main output signal at 4·43 MHz, of about 12% or 1 dB.

Since, at the time of writing, no precise Q measurements for the glass 239 at 4·43 MHz are available we will subtract all the calculated losses from the measured overall loss to obtain an approximation for the medium losses and thereby for the Q of the glass. Since our terminations are symmetrical, an insertion loss of 8 dB signifies 14 dB loss between V_l and E, or

$$\frac{V}{E} = 0{\cdot}2.$$

We now have

$$x \times 0{\cdot}404 \times 0{\cdot}88 \times 0{\cdot}75 = 0{\cdot}2, \tag{3.4}$$

where we have written 0·75 for the loss due to beam divergence (2·5 dB) and x for the medium loss. There results

$$x = 0{\cdot}75$$

and, using

$$x = \exp\left(-\frac{\pi n}{Q}\right),$$

where n is the length of the propagation path divided by the wavelength,

$$Q \approx 3000 \qquad \text{(glass 239, freq. 4·43 MHz)}.$$

The treatment just given is not, of course, recommended as a method of determining Q; our object was only to obtain a fair estimate of the way the losses are distributed. In making up this balance of losses we are justified in neglecting the transducer losses and the solder-band losses. The latter are small, because the solder-bond length is so small. However, they could conceivably become of interest in another respect: even though the energy lost in the solder bond is relatively small, the temperature of the bond will be higher than that of the surrounding parts. Where much more than the usual amount of power would be required, the bond temperature would be one of the factors limiting the available output.

The subject of obtainable bandwidth will be treated in detail in the chapter on transducers, and therefore we will not dwell long on it here. In that chapter we deduce the following value for the load and source resistance R which gives maximum bandwidth:

$$\frac{R_m}{R} = 0{\cdot}33.$$

Experimentally we have determined this value of R to be 150 Ω. Since the glass impedance on the electrical side is seen as 58·8 Ω the experimentally found ratio of R_m to R is 0·39, a good match with the ratio derived experimentally.

Remarks

It follows from what has just been derived that the reflection coefficient for the acoustic midband-frequency radiation energy, reaching an unbacked transducer, does not directly depend upon the ratio ζ, the ratio of medium impedance to transducer impedance. We can also explain this by noting that for frequencies near the midband frequency the transducer, as seen by the sound wave, represents to a good approximation a transmission line of half a wavelength long. Thus, whatever the value of the impedance of the transducer

material is, the sound wave sees the electrical load, (or source) impedance. By making the load (source) resistive and by changing its value, the corresponding reflection coefficient may be given any value between —1 and 1. The condition which makes ϱ zero ($R_S = R_L = R_m$) is generally not the condition for maximum bandwidth, so that usually a designer will have to choose between optimum bandwidth and minimal reflections. It should be added however that in our case the transducer-facet area is larger than the transducer area. This fact has to some extent been made use of as follows. The external resistances were chosen to yield maximum bandwidth, which made them larger than R_m. It follows that the reflection coefficient is positive. For those areas (outside the transducer) where there is a glass-air boundary we may expect a negative reflection coefficient so that the two reflection contributions tend to cancel.

The measured attenuation curves for the main output signal as well as for the 3τ reflections are given in fig. 3.7.

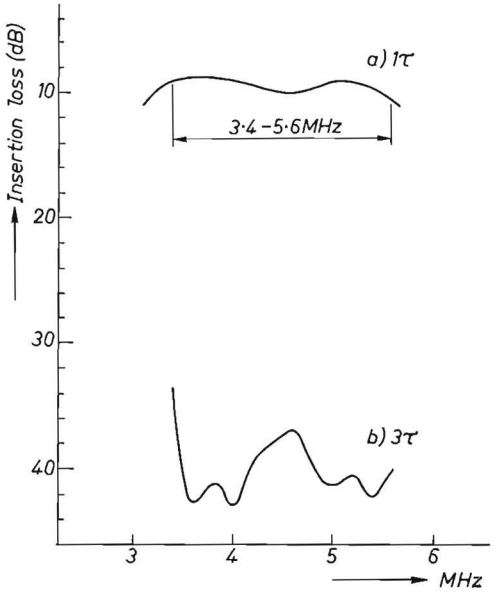


Fig. 3.7. Insertion-loss vs frequency curves of PAL delay line; (*a*) main signal (1τ) signal, (*b*) 3τ reflection.

3.6.2. *Delay variation with temperature*

The temperature drift of the phase delay is of course largely determined by the properties of the propagation medium. The propagation body of the DL1 is made of a potash-lead-silicate glass, developed for the purpose by the Philips Glass Development Centre [3-28,29]).

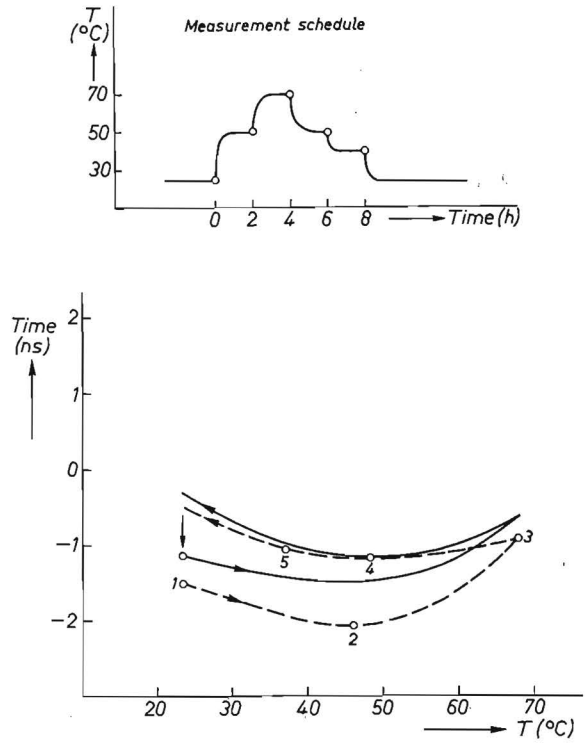


Fig. 3.8. Phase-delay-time vs temperature curves measured on two consecutive days; - - - - - - - - - first day, ———— second day.

The relation between the relative variation of the delay time ($\Delta\tau/\tau$) and temperature is approximately given by

$$\frac{\Delta\tau}{\tau} = 0{\cdot}04\,(T - T_0)^2\,10^{-6}. \tag{3.5}$$

This relationship will not be found if points on the curve are determined in "quick" succession, that is within one day or even within a few days. Figure 3.8 shows a succession of measurements together with the time elapsed since the start of the measurement cycle. It is seen that the delay time, after a full cycle, does not return to its original value. The difference will disappear slowly if the glass is left at the starting temperature, complete elimination of this difference taking a few days. There exist after-effects in the glass, which are still subjects of study [3–29]). For quick and large thermal variations the resulting delay-time deviations will exceed the values given by (3.5). Thus, this formula is not very useful for specification purposes. For specification of the temperature stability of the delay line it is more practical to state the values which will not be exceeded within certain temperature intervals. The specification for the DL1 regarding

this property, reads: "the temperature drift of phase delay will be less than plus or minus 5 ns with respect to the phase delay at 25 °C during the following heat treatment: warm up linearly from 20 to 50 °C in three hours and keep at 50 °C for two more hours". This specification holds for the DL1 as a whole, so that it includes the variation caused by the ceramic transducers.

3.6.3. *Phase-delay accuracy*

We have already briefly described the delay adjustment in sec. 3.4. We have also shown (sec. 3.5.3) that this adjustment is not feasible in a simple bar type of delay line. The delay adjustment of the DL1 delay line can be done with relative ease and the accuracy obtainable is sufficient.

The initial delay time should of course be too long. During grinding, the delay is monitored electrically by means of the delay line's own transducers. First the group delay is measured; this phase of the grinding operation is continued until the group delay differs by less than about 100 ns from the desired group-delay time. Then the electrical monitoring equipment is switched over to phase measurement and grinding is continued until the subcarrier phase response equals $m\pi$. Thus, phase accuracy is given preference over group-delay accuracy. The multiple m is so chosen that the group delay nearest 64 μs is obtained. As we have discussed before, m may be an even as well as an odd integral number; thus 2×283, $2\times283{\cdot}5$, 2×284, etc. are acceptable values for m. A phase difference of π radians corresponds, at the subcarrier frequency to about 113 ns. Thus it should always be possible to find a value of m for which the group delay differs by less than 57 ns from the desired value. In this way it has turned out to be possible to satisfy both the phase-response requirement and the group-delay requirement. In the laboratory phase accuracies of better than 1 ns have been obtained. For the mass-produced delay line the specified tolerance is ± 3 ns. This deviation can, if necessary, conveniently be further reduced by a phase adjustment in the receiver.

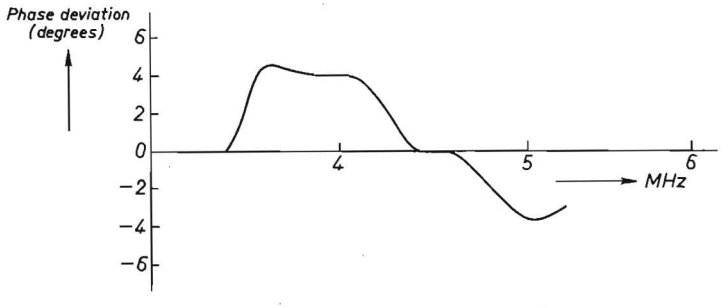


Fig. 3.9. Measured deviation from ideal response.

3.6.4. *Dispersion*

In fig. 3.9 the measured phase deviation is shown as a function of frequency for a mass-produced DL1. The ordinate is the deviation of the actual phase response from the ideal phase response, the latter being given by a straight line going through a point $m\pi$, and having a slope of 64 μs.

REFERENCES

3-1) Blackburn, Components handbook, Radiation laboratory series No. 17, McGraw-Hill Book Company, Inc., Ch. 6.
3-2) A. M. Turner, R.C.A. Rev. **10**, 477-489, 1949.
3-3) P. M. Prache, Câbles Transm. **17**, 14-36, 1963.
3-4) V. S. Martinov and E. D. Bauman, Telecommunications and Radio Engineering **3**, 39-44, 1964.
3-5) W. J. Hannan, J. F. Schanne and D. J. Woywood, I.E.E.E. Trans. **MIL-9**, 246-254, 1965.
3-6) J. S. Palfreeman, Ultrasonics **3**, 1-8, 1965.
3-7) D. L. Arenberg, I.R.E. Natl Conv. Rec. **2**, Part 6, 63-72, 1954.
3-8) J. H. Eveleth, Proc. I.E.E.E. **53**, 1406-1428, 1965.
3-9) W. P. Mason, Proc. Inst. Radio Engrs **50**, 1374-1384, 1962.
3-10) C. F. Brockelsby, J. S. Palfreeman and P. W. Gibson, Ultrasonic delay lines, London Iliffe Books Ltd., 1963.
3-11) W. P. Mason (ed.), Physical acoustics, Academic Press, New York, London, 1964, Volume I, Part A.
3-12) P. and J. Curie, C.R. Acad. Sci. Paris **91**, 294-295, 1880.
3-13) M. P. Langevin, Brevet Nr. 505703 (1918); see also Nr. 576281 (1924) and Nr. 622035 (1926).
3-14) E. Klein, J. acoust. Soc. Am. **5**, 601-604, 1948.
3-15) O. E. Buckley, J. appl. Phys. **8**, 40-47, 1937.
3-16) H. B. Huntington, A. G. Emslie and V. W. Hughes, J. Franklin Inst. **245**, 1-23, 1948.
3-17) A. G. Emslie, H. B. Huntington, H. Shapiro and A. E. Benfield, J. Franklin Inst. **245**, 101-115, 1948.
3-18) F. Kruse, Telefunken GmbH, DRP 893059 (1940).
3-19) A. C. Keller, Trans. A.I.E.E. **66**, 1217-1230, 1947.
3-20) W. P. Mason, Proc. Inst. Radio Engrs **35**, 1005-1012, 1947.
3-21) S. Roberts, Phys. Rev. **71**, 890-895, 1947.
3-22) R. B. Grag, U.S. Patent No. 2,486,560 (1946).
3-23) W. L. Cherry Jr. and Robert Adler, Phys. Rev. **72**, 981-982, 1947.
3-24) G. Shirane and S. Hoshino, J. phys. Soc. Japan **6**, 265-270, 1951.
3-25) B. Jaffe, R. S. Roth and S. Marzullo, J. appl. Phys. **25**, 809-810, 1954.
3-26) B. Jaffe, R. S. Roth and S. Marzullo, J. Res. natl Bur. Stand. **55**, 239, 1955.
3-27) C. F. Brockelsby and J. S. Palfreeman, Philips tech. Rev. **25**, 234-252, 1963/64.
3-28) A. L. Zijlstra, Dutch Patent No. 6504 829 (1965).
3-29) A. L. Zijlstra and C. M. van der Burgt, Ultrasonics **5**, 29-38, 1967.
3-30) W. Bruch, Telefunken-Zeitung **38**, 37, 1965.
3-31) A. Köhler, Int. Elektron. Rdsch. **1**, 13-15, 1967.
3-32) F. Th. Backers and F. A. L. Suijkerbuijk, Dutch Patent No. 6604240 (1966).
3-33) M. Ward, Product Engng **27**, 135-140, 1956.
3-34) A. Rothbart and L. Rosenberg, I.R.E. Trans. **PGUE-6**, 32, 1957.
3-35) S. Goldstein, I.E.E.E. Trans. **UE-10**, 56-71, 1963.
3-36) G. G. Scarrott and R. Naylor, Proc. Instn elect. Engrs **103**, Part B, Supplement Nr. 3, 497-508, 1956.
3-37) A. Rothbart, Proc. Inst. Radio Engrs, XLVII **6**, 1153-1154, 1959.
3-38) W. Bruch, Electron. Engng **36**, 606-611, 1964.
3-39) F. Th. Backers and H. L. Swaluw, Dutch patent appl. No. 6804788 (1968).
3-40) A. H. Meitzler, I.R.E. Trans. **UE-7**, 35-43, 1960.
3-41) A. H. Meitzler, I.R.E. Trans. **UE-9**, 30-37, 1962.

3-42) J. Miklowitz, Appl. Mech. Rev. **13**, 865-878, 1960.
3-43) A. E. H. Love, A treatise on the mathematical theory of elasticity, Dover, New York, 1892.
3-44) H. Kolsky, Stress waves in solids, Oxford Univ. Press., 1953.
3-45) R. N. Thurston and P. Anreatch, I.R.E. Conv. Rec. **3**, Part 9, 45-54, 1955.
3-46) R. N. Thurston, I.R.E. Trans. **UE-7**, 16-25, 1960.
3-47) A. O. Williams Jr., J. acoust. Soc. Am. **23**, 1-6, 1951.
3-48) H. Seki, A. Granato and R. Truell, J. acoust. Soc. Am. **28**, 230-238, 1956.
3-49) R. Bass, J. acoust. Soc. Am. **30**, 602-605, 1958.
3-50) Y. Fujii and K. Yamada, J. acoust. Soc. Am. **40**, 249-251, 1966.
3-51) K. Yamada and Y. Fujii, J. acoust. Soc. Am. **40**, 1193-1194, 1966.

4. DELAY-LINE CHARACTERISTICS

4.1. Theoretical survey

It is the purpose of this section to derive the formulas and equivalent circuits (of various degrees of exactness) which will be used in the next three sections.

Even if one exercises restraint in the use of symbols and indexes, a great many of these are needed for a theoretical discussion of piezoelectric transducers. For a discussion on nomenclature the reader is referred to a recent book by Zwikker [4-1]). We have tried to follow the recommendations approved by the Commission for Symbols, Units and Nomenclature (S.U.N. Commission) of the International Union of Pure and Applied Physics (I.U.P.A.P.) [4-2]). Wherever the S.U.N.-commission document makes no specific recommendations we have tried to be in accordance with I.R.E. Standards [4-3,4,5,6]).

We consider the electromechanical behaviour of a ceramic transducer (fig. 4.1) having the shape of a thin plate, the plate being polarized perpendicular to the thickness direction. The direction of the polarization is the 3-direction. The two major faces ($x = 0$ and $x = l$) are covered with electrode layers of negligible thickness. One of the major faces of this transducer is bonded to a propagation medium, the other is left free. The bond is again of negligible thickness. Across the electrodes, an alternating voltage of amplitude E and angular frequency ω

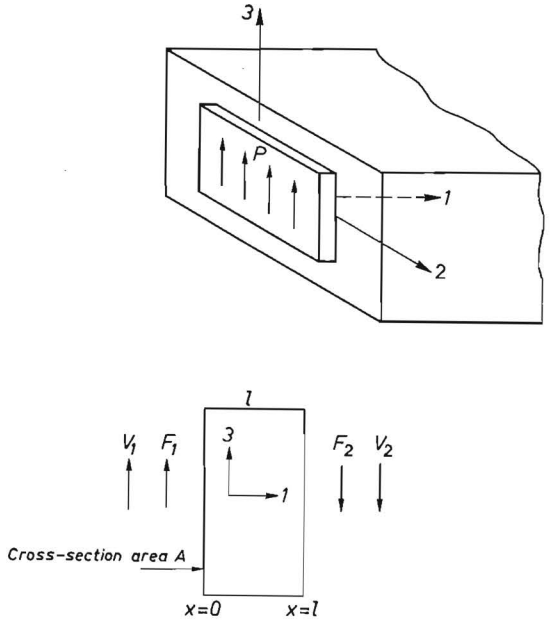


Fig. 4.1. Thickness-shear transducer.

is applied. The transducer medium is assumed to be free of electrical and mechanical losses.

The components of the elastic displacement are u_1, u_2 and u_3. The six stress components are called σ_1, σ_2, . . ., σ_6, where

$$\sigma_4 = \sigma_{23}, \qquad \sigma_5 = \sigma_{13}, \qquad \sigma_6 = \sigma_{12}.$$

The six strain components are $e^{(1)}$, $e^{(2)}$, . . ., $e^{(6)}$, where

$$e^{(4)} = \frac{\partial u_3}{\partial x_2} + \frac{\partial u_2}{\partial x_3},$$

$$e^{(5)} = \frac{\partial u_1}{\partial x_3} + \frac{\partial u_3}{\partial x_1},$$

$$e^{(6)} = \frac{\partial u_2}{\partial x_1} + \frac{\partial u_1}{\partial x_2},$$

The lateral dimensions of the transducer are assumed to be so large that the various electrical and mechanical quantities do not depend on x_2 and x_3. This in principle leaves $e^{(1)}$, $e^{(5)}$ and $e^{(6)}$ as possible strains. We further assume the electric-displacement vector to have the 1-direction. Since $\nabla D = 0$ in the transducer material, it follows that D_1 in the transducer is independent of the space variables; it may be a function of time however. The D_1 component generates, through the piezoelectric constant h_{15}, σ_5 stresses, and/or $e^{(5)}$ strains; it therefore seems reasonable to assume that all strains except $e^{(5)}$ are zero. Of the possible sets of piezoelectric relations we choose:

$$\begin{bmatrix}\sigma_1\\ \sigma_2\\ \sigma_3\\ \sigma_4\\ \sigma_5\\ \sigma_6\end{bmatrix} = \begin{bmatrix} {c_{11}}^D & {c_{12}}^D & {c_{13}}^D & 0 & 0 & 0\\ {c_{12}}^D & {c_{11}}^D & {c_{13}}^D & 0 & 0 & 0\\ {c_{13}}^D & {c_{13}}^D & {c_{33}}^D & 0 & 0 & 0\\ 0 & 0 & 0 & {c_{44}}^D & 0 & 0\\ 0 & 0 & 0 & 0 & {c_{44}}^D & 0\\ 0 & 0 & 0 & 0 & 0 & {c_{66}}^D \end{bmatrix} \begin{bmatrix}e^{(1)}\\ e^{(2)}\\ e^{(3)}\\ e^{(4)}\\ e^{(5)}\\ e^{(6)}\end{bmatrix} - \begin{bmatrix} 0 & 0 & h_{31}\\ 0 & 0 & h_{31}\\ 0 & 0 & h_{33}\\ 0 & h_{15} & 0\\ h_{15} & 0 & 0\\ 0 & 0 & 0 \end{bmatrix} \begin{bmatrix}D_1\\ D_2\\ D_3\end{bmatrix}$$

and

$$\begin{bmatrix}E_1\\ E_2\\ E_3\end{bmatrix} = - \begin{bmatrix} 0 & 0 & 0 & 0 & h_{15} & 0\\ 0 & 0 & 0 & h_{15} & 0 & 0\\ h_{31} & h_{31} & h_{33} & 0 & 0 & 0 \end{bmatrix} \begin{bmatrix}e^{(1)}\\ e^{(2)}\\ e^{(3)}\\ e^{(4)}\\ e^{(5)}\\ e^{(6)}\end{bmatrix} + \begin{bmatrix} {\beta_{11}}^S & 0 & 0\\ 0 & {\beta_{11}}^S & 0\\ 0 & 0 & {\beta_{33}}^S \end{bmatrix} \begin{bmatrix}D_1\\ D_2\\ D_3\end{bmatrix}.$$

The appearance of the matrices is determined by the fact that the polarized ceramic material belongs to the crystal class C_{6v} or $6mm$ [4–5]). From these

equations it also follows that if $e^{(5)}$ is the only non-zero strain, then σ_5 is the only non-zero stress. The last two equations now reduce to

$$\sigma_5 = c_{44}{}^D e^{(5)} - h_{15} D_1 \tag{4.1}$$

and

$$E_1 = -h_{15} e^{(5)} + \frac{1}{\varepsilon_{11}{}^e} D_1, \tag{4.2}$$

where $1/\varepsilon_{11}{}^e$ has been written for $\beta_{11}{}^e$.

Introduce the boundary values of the particle velocity V_1 and V_2 as follows;

$$V_1 \exp(j\omega t) = \left(\frac{\partial u_3}{\partial t}\right)_{x=0}$$

and

$$V_2 \exp(j\omega t) = -\left(\frac{\partial u_3}{\partial t}\right)_{x=l}.$$

Let the boundary values of the shear forces which the adjoining media exert on the transducer be F_1 and F_2:

$$F_1 = -A(\sigma_5)_{x=0}$$

and

$$F_2 = -A(\sigma_5)_{x=l}.$$

Introduce

$$V^D = (c_{44}{}^D/\varrho)^{1/2}, \tag{4.3}$$

$$I = j\omega A D_1, \tag{4.4}$$

$$Z_0 = A\varrho V^D, \tag{4.5}$$

where A is the area of the cross-section of the transducer and ϱ its density; I is the current flowing to and from the external circuit, and Z_0 is the acoustic shear impedance of the medium for constant dielectric displacement. We will discuss sinusoidal variations; all capital letters representing variables, such as I, F_1 and V_2 will be considered to be amplitudes; the common factor $\exp(j\omega t)$ will be omitted. We have

$$\frac{\partial \sigma_5}{\partial x} = \varrho \frac{\partial^2 u_3}{\partial t^2}. \tag{4.6}$$

Solving (4.6) and satisfying (4.1) and the boundary conditions, gives the following sinusoidal solutions:

$$F_1 = -\frac{jZ_0}{\tan(kl)} V_1 - \frac{jZ_0}{\sin(kl)} V_2 + \frac{h_{15}}{j\omega} I$$

and

$$F_2 = -\frac{jZ_0}{\sin(kl)} V_1 - \frac{jZ_0}{\tan(kl)} V_2 + \frac{h_{15}}{j\omega} I, \tag{4.7}$$

where

$$k = \frac{2\pi}{\lambda} = \frac{\omega}{V^D}. \tag{4.8}$$

The equations (4.7) are transformed into a more useful form by making use of the relation

$$\frac{1}{\tan(kl)} = \frac{1}{\sin(kl)} - \tan\frac{kl}{2}.$$

The voltage E is obtained by integrating (4.2). If we also introduce the shear-clamped capacitance

$$C_0{}^S = \frac{A\,\varepsilon_{11}{}^e}{l} \tag{4.9}$$

the final result will be

$$\begin{aligned} F_1 &= \left(jZ_0 \tan\frac{kl}{2} + \frac{Z_0}{j\sin(kl)}\right) V_1 + \frac{Z_0}{j\sin(kl)} V_2 + \frac{h_{15}}{j\omega} I, \\ F_2 &= \frac{Z_0}{j\sin(kl)} V_1 + \left(jZ_0 \tan\frac{kl}{2} + \frac{Z_0}{j\sin(kl)}\right) V_2 + \frac{h_{15}}{j\omega} I, \\ E &= \frac{h_{15}}{j\omega} V_1 + \frac{h_{15}}{j\omega} V_2 + \frac{I}{j\omega C_0{}^S}. \end{aligned} \tag{4.10}$$

An equivalent circuit for the equations (4.10) is clearly given by fig. 4.2. The transformer ratio of the ideal electromechanical transformer shown is $1 : \phi$ (impedance ratio $1 : \phi^2$) where

$$\phi = h_{15} C_0{}^S. \tag{4.11}$$

In fig. 4.3*a* the acoustic impedance Z_1 of the medium adjoining the face $x = 0$ has been introduced; Z_1 is defined by

$$Z_1 = A\varrho_1 V_1,$$

where ϱ_1 and V_1 are the density and the shear-wave velocity of medium 1 ($x < 0$). If Z_2 be the acoustic impedance ($Z_2 = A\varrho_2 V_2$) of the medium 2 ($x > l$) and if we assume medium 1 to be air (for which the impedance is negligibly small), then fig. 4.3*a* may be transformed in a well-known manner [4–7]) (see fig. 4.3*b*) into fig. 4.3*c*. The defintions of Z_1 and Z_2 of course imply that the states of vibration in the media 1 and 2, near the transducer faces, may be approximated by plane waves. This assumption is a logical extension of our

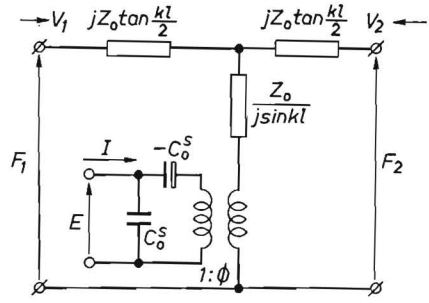


Fig. 4.2. Equivalent circuit for thickness-shear transducer.

earlier assumption that the vibration of the transducer medium was one-dimensional.

The frequency which makes $kl/2$ equal to $\pi/2$ is called the antiresonance frequency f_a, in accordance with the standardizations referred to before[4–4]). It follows that the wavelength at the frequency f_a is given by

$$\lambda_a = 2l. \tag{4.12}$$

At this frequency, the impedance of the freely ($Z_1 = Z_2 = 0$) vibrating transducer is infinite; this follows from an examination of fig. 4.3*c*, which at the frequency f_a reduces to a parallel circuit of $C_0{}^S$ and $-C_0{}^S$.

For frequencies not too far from f_a the equivalent circuit of fig. 4.3*c* may be approximated by a lumped-element circuit if the impedance $2Z_0/j \tan (kl/2)$ is replaced by a series LC circuit with the values

$$L_{\text{mech}} = \frac{\pi Z_0}{2\omega_a} = \tfrac{1}{2} Al\varrho$$

and (4.13)

$$C_{\text{mech}} = \frac{2}{\pi Z_0 \omega_a},$$

and the impedance $2jZ_0 \tan (kl/2)$ is replaced by a parallel LC circuit with

$$L'_{\text{mech}} = \frac{8Z_0}{\pi\omega_a}$$

and (4.14)

$$C'_{\text{mech}} = \frac{\pi}{8Z_0\omega_a}.$$

The result is given in fig. 4.4, where the ideal electromechanical transformer has also been eliminated by transforming the elements to the electrical side. We will

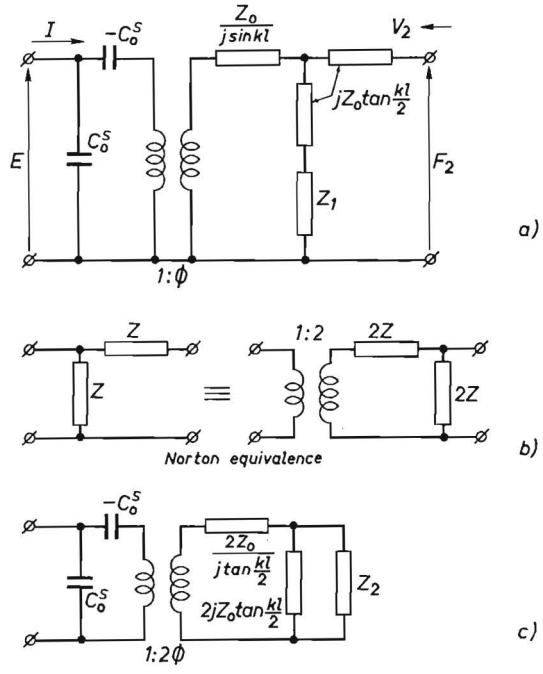


Fig. 4.3. The Norton equivalence is used to transform the circuit *a* (with $Z_1 = 0$) into that of *c*.

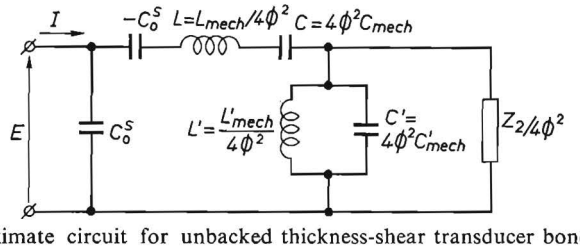


Fig. 4.4. Approximate circuit for unbacked thickness-shear transducer bonded to medium with acoustic impedance Z_2; all elements transformed to electrical side. Approximations are best for frequencies around $f_a = V^D/2l$.

use this circuit later for an approximate investigation of transducer responses. It would be possible to obtain a better lumped-element approximation than is afforded by fig. 4.4; for such an approach, the reader is referred to an article by Müser and Bittel [4–8]). We will be satisfied with the approximation of fig. 4.4, however, since we intend to employ the circuit of fig. 4.3*c* for exact calculations.

We now introduce the electromechanical coupling factor k_{15}; this may be done in a manner which makes its physical meaning apparent. See for example pages 35, 36 of the book by Brockelsby, Palfreeman and Gibson [4–7]) or an article by Bechmann [4–9]). Here, for the sake of convenience, k_{15} will be defined by the equation

$$\varepsilon_{11}{}^{\sigma}(1 - k_{15}{}^{2}) = \varepsilon_{11}{}^{e}, \tag{4.15}$$

where $\varepsilon_{11}{}^{\sigma}$ is the free ($\sigma_5 = 0$) dielectric constant and $\varepsilon_{11}{}^{e}$ the clamped ($e^{(5)} = 0$) constant. From the equations (4.1), (4.2) and (4.15) it follows that

$$k_{15} = h_{15}\left(\frac{\varepsilon_{11}{}^{e}}{c_{44}{}^{D}}\right)^{1/2}. \tag{4.16}$$

We now complete this theoretical introduction by deriving a few relations which are then used to put both the circuit of fig. 4.4 and the exact circuit of fig. 4.3*c* into a different form.

From the equations (4.3), (4.5), (4.8), (4.11), (4.12) and (4.16) we may deduce the relation

$$\frac{Z_0}{4\phi^2} = \frac{1}{8k_{15}{}^{2} f_a C_0{}^{S}}. \tag{4.17}$$

Thus, (4.17) does not contain the approximations of equations (4.13) and (4.14).

If we introduce

$$a = \frac{1}{8k_{15}{}^{2} f_a C_0{}^{S}} \tag{4.18}$$

and

$$\zeta = \frac{Z_2}{Z_0}, \tag{4.19}$$

then the circuit of fig. 4.3*c* may be brought into the form shown in fig. 4.5. The latter circuit will be used as a basis for exact computations in sec. 4.4. The circuit to be used in sec. 4.4 is obtained as follows. Using (4.17) and (4.18) the series-circuit values in fig. 4.4 can be written:

$$L = \frac{\pi}{2}\frac{a}{\omega_a}$$

and (4.20)

$$C = \frac{2}{\omega_a \pi a}.$$

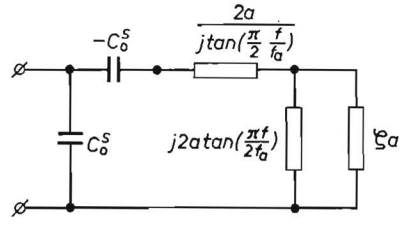


Fig. 4.5. Equivalent circuit of unbacked thickness-shear transducer bonded to medium with acoustic impedance $Z_2 = \zeta Z_0$.

In fig. 4.4 we now also omit the parallel circuit $L'C'$. Unless ζ is fairly large this is not a severe approximation. In the early literature on this subject the negative capacitance was often omitted since k_{15} was usualy small enough to make this an allowable procedure. In this connection it is interesting to point out, that if in fig. 4.4 as well as in fig. 4.5 the element $-C_0{}^S$ is not omitted, then the impedance of the freely vibrating transducer ($Z_1 = Z_2 = 0$) is infinite at the frequency f_a, whereas, if this element is neglected, the impedance under the same conditions is found to be zero. Of course, for small values of k_{15}, the frequencies causing a minimum and a maximum value for Z_{free} are close together and the matter is of little practical importance; in this field, however, it would seem advisable to guard against sources of confusion.

Since we are dealing with high values of k_{15}, we will not omit the element $-C_0{}^S$; it is lumped together with C (4.20) to give

$$C_{\text{eff}} = \frac{2\,C_0{}^S}{\omega_a\,\pi a C_0{}^S - 2}. \tag{4.21}$$

As a result we now have the approximation circuit of fig. 4.6 in which L_p represents an externally connected coil, the inductance of which will be chosen later.

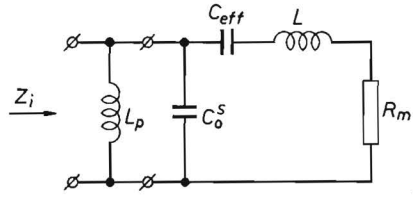


Fig. 4.6. Approximate circuit for unbacked thickness-shear transducer bonded to medium with acoustic impedance ζZ_0; $R_m = \zeta a$, $L = \frac{\pi}{2}\frac{a}{\omega_a}$, $C_{\text{eff}} = \frac{2\,C_0{}^S}{\omega_a \pi a C_0{}^S - 2}$; C_{eff} is the series equivalent of $-C_0{}^S$ and C.

4.2. Approximate examination of transducer-pair responses

In this section as well as in sec. 4.3 it is our purpose to calculate or compute overall delay-line responses such as the attenuation-frequency characteristic and the phase-frequency characteristic. The effect which the acoustic-wave propagation has on these responses will, for the moment, not be considered, so it is really transducer-pair responses which are being discussed.

From fig. 4.5 and eq. (4.18) we conclude that the parameters describing one unbacked transducer are $1/\omega_a C$, k_{15} and ζ; the response is further determined by the external elements L and R; consider finally that two transducers and two external circuits are employed and it becomes clear that a rather large number of parameters enter the case. The number of cases which one would like to

examine can easily become impractically large. To present a general survey of the response for a number of parameter values, so that we are not confined to the case of the delay line type DL1 only, and yet to restrict the number of cases, we have introduced some assumptions and we have searched for parameter combinations which are in some way meaningful.

First we assume that both transducers are tuned externally by parallel coils. We also assume mechanical and electrical symmetry, that is, the transducers have identical dimensions, the external parallel coils just mentioned have equal self-inductances and the source and load resistances are equal (L_p and R).

In addition we make a choice for the value of L_p. Let Z_i (fig. 4.6) be the electrical impedance looking into the transducer (L_p included). We choose the value of L_p such that the absolute value of Z_i will be a symmetrical function of log ω around a certain frequency ω_0'. This may be accomplished by choosing

$$L_p C_0{}^S = LC'$$

or

$$L_p = \frac{\pi a}{\omega_a(\omega_a \pi a C_0{}^S - 2)} \tag{4.22}$$

or

$$j\omega L_p = \frac{ja\{(\pi/2)\, f/f_a\}}{\pi^2/8k_{15}{}^2 - 1}.$$

It follows that

$$\omega_0{}' = \omega_a\left(1 - \frac{2}{\omega_a \pi a C_0{}^S}\right)^{1/2} = \omega_a\left(1 - \frac{8k_{15}{}^2}{\pi^2}\right)^{1/2}. \tag{4.23}$$

Finally we assume that, for the purpose of this section, the property of main interest is the 3-dB bandwidth of the delay line and therefore we search for the value of R making this bandwidth a maximum, R of course being a function of the remaining parameters. We spend the remainder of this section determining this resistance function by means of an approximate analysis.

We first derive an expression for the transfer. Figure 4.7 shows input transducer and output transducer separated by the propagation medium. Let

$$\gamma = \frac{I_1}{E_S}. \tag{4.24}$$

The mechanical shear force generated at the input side then equals $R_m I_1$. This signal propagates: we assume that the delay line, as seen from the output side, may be represented by a generator of voltage $2R_m I_1$ and internal impedance R_m. The factor 2 of course reflects the fact that the propagation medium is replaced by its Thévenin equivalent. It also signifies that this medium is assumed to give

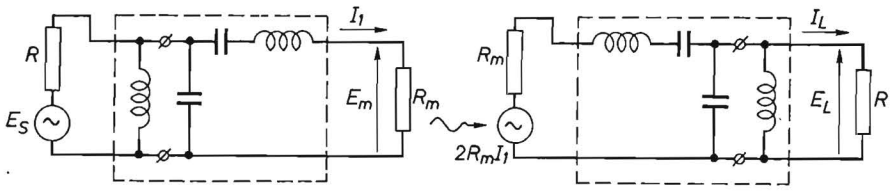


Fig. 4.7. Transducer-pair representation.

no loss and no distortion. The reciprocity theorem requires that

$$\gamma = I_L/2R_mI_1, \tag{4.25}$$

so that the transfer

$$\frac{E_L}{E_S} = 2\,\gamma^2\,RR_m. \tag{4.26}$$

The circuits shown within the dashed lines in fig. 4.7 contain the approximate circuits of fig. 4.6. For the sake of clarity we introduce

$$\omega_0'L = q, \tag{4.27}$$

$$\omega_0'C_0^S = p, \tag{4.28}$$

$$V = \frac{\omega}{\omega_0'} - \frac{\omega_0'}{\omega} \tag{4.29}$$

and

$$R = rR_m = r\zeta a. \tag{4.30}$$

Let γ_0 be the value of γ for $V = 0$, then it may be shown that

$$\left|\frac{\gamma}{\gamma_0}\right|^2 = \frac{(1+r)^2}{(1+r-pqrV^2)^2 + (q/\zeta a + pr\zeta a)^2V^2}. \tag{4.31}$$

It can also be shown that

$$\begin{aligned} p &= \frac{(1-8k_{15}^2/\pi^2)^{1/2}}{(8k_{15}^2/\pi^2)\,\pi a/2}, \\ q &= \frac{\pi a}{2}\left(1-\frac{8k_{15}^2}{\pi^2}\right)^{1/2}, \\ pq &= \frac{\pi^2}{8k_{15}^2}\left(1-\frac{8k_{15}^2}{\pi^2}\right). \end{aligned} \tag{4.32}$$

Thus (4.31) shows the normalized voltage transfer as a function of the coupling

factor k_{15}, the external resistance, the "matching factor" ζ and the relative frequency ω/ω_0'. We finally introduce

$$r = 1/u. \tag{4.33}$$

Analysis of (4.31) reveals the following facts. For values of u larger than u_1, where

$$u_1 = \left(\frac{\zeta^2}{{k_{15}}^2} - \frac{\zeta^4}{4{k_{15}}^4} \right)^{1/2} \tag{4.34}$$

the overall response (4.31) is single-peaked while for u smaller than u_1 the response is double-peaked. For

$$u < u_2,$$

where

$$u_2 = -\frac{c}{2}\frac{\zeta^2}{{k_{15}}^2} + \frac{\zeta^2}{2{k_{15}}^2}\left(c^2 - 1 + \frac{4(1-c)}{\zeta^2/{k_{15}}^2} \right)^{1/2} \tag{4.35}$$

with $c = (1 - \frac{1}{2}\sqrt{2})^{1/2}$,

the response is double-peaked with a ratio of maximum to central response larger than $\sqrt{2}$. The curves $u_1(\zeta/k_{15})$ and $u_2(\zeta/k_{15})$ are shown in fig. 4.8. Within the two regions $u > u_1$ and $u_2 < u < u_1$ we define the 3-dB bandwidths as indicated in fig. 4.8 and call them BW1 and BW2, respectively. The values of u which maximize these bandwidths are now to be determined. We distinguish two regions: (a) $\zeta^2/{k_{15}}^2 < 2\sqrt{2}$ and (b) $\zeta^2/{k_{15}}^2 > 2\sqrt{2}$ $((2\sqrt{2})^{1/2} \approx 1{\cdot}68)$.

(a) $\zeta^2/{k_{15}}^2 < 2\sqrt{2}$

In this region, it is found that

for $u \geqslant u_1$: $\partial/\partial u\,(\mathrm{BW1}) < 0$ and
for $u_2 < u < u_1$: $\partial/\partial u\,(\mathrm{BW2})$ is a monotonically decreasing function of u, which is negative on $u = u_1$.

It follows that we will find no maximum of BW1 in the region $u > u_1$ and $\zeta^2/{k_{15}}^2 < 2\sqrt{2}$. It also follows that in the region $u_2 < u < u_1$ and $\zeta^2/{k_{15}}^2 < 2\sqrt{2}$ we may find, for a given value of ζ/k_{15}, one, but no more than one value of u which makes BW2 a maximum. A number of these maximum values have been determined by computer: they lie on the curve $u = u_{m_2}$. This curve crosses the curve $u = u_2$ at $\zeta/k_{15} \approx 0{\cdot}67$ and for lower values of ζ/k_{15}, $u_{m_2} < u_2$. It would have been possible to define a bandwidth function BW3 for that region $(u < u_2)$ and to analyze it; this was not done since the transfer-curve shape there was considered unsatisfactory (maximum response more than 3 dB above minimum response).

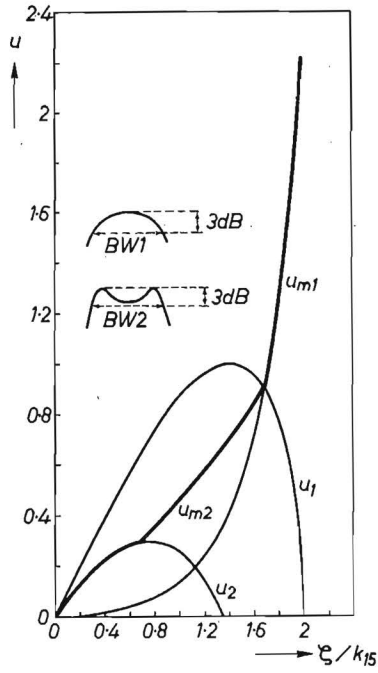


Fig. 4.8. Approximate analysis of transducer-pair response. For a given value of ζ/k_{15}, maximum bandwidth is obtained if u lies on the fat curve $u_2 - u_{m2} - u_{m1}$;

$$u = \frac{\text{electr. equivalent of radiation resistance}}{\text{load (or source) resistance}} = \frac{R_m}{R}.$$

For $u > u_1$, the response is single-peaked,
For $u < u_1$, the response is double-peaked,
For $u < u_2$, the max.-to-min. ratio in the response is greater than $\sqrt{2}$.

(b) $\zeta^2/k_{15}^2 > 2\sqrt{2}$

For this region the analysis gives the following results:

for $u \leqslant u_1$: $\partial/\partial u\,(\mathrm{BW2}) > 0$,
for $u > u_1$: $\partial/\partial u\,(\mathrm{BW1})$ is a monotonically decreasing function of u which is positive on $u = u_1$ and becomes negative for u large enough. It follows that for $\zeta^2/k_{15}^2 > 2\sqrt{2}$ there will be no maximum of BW2 below the curve $u = u_1$, while above that curve, for a given value of ζ/k_{15}, there will be one, but not more than one value of u making BW1 a maximum. The latter values are found to be on the curve

$$u = u_{m_1} = \frac{g}{8}[(g\sqrt{2} - 4) + \{(g\sqrt{2} - 4)^2 + 16(\sqrt{2} - 1)\}^{1/2}], \quad (4.36)$$

where we have written g for ζ^2/k_{15}^2. To recapitulate: if we vary ζ/k from 0 to ∞ the optimum values of u (values causing maximum bandwidth) will follow

the fat-curve sections u_2, u_{m_2} and u_{m_1}. The corresponding responses are double-peaked, double-peaked and single-peaked, respectively. These results will be used in the next section.

4.3. Computations of transfer responses and reflection coefficients

In this section, computed transducer-pair characteristics will be presented. Since use is made of a computer, there is little need to utilize the approximate circuits; the exact circuit of fig. 4.5 will be the base for computations. The choice of parameter values and the restriction of the number of cases has been described in the previous section. The parameter values for the computed cases are given in table 4-I. Four values of k_{15} and two values of ζ were chosen; one of the latter ($\zeta = 0{\cdot}45$) is the impedance ratio for the DL1 which is derived in the next section. The four values of the coupling factor cover fairly well the range which may be expected in ceramic transducers. There result eight values of ζ/k_{15} and these have been combined with resistance ratios which were taken from the optimal curves in fig. 4.8.

TABLE 4-I

Computed cases

fig.	ζ	k_{15}	u	ζ/k_{15}
4.9*a*	0·45	0·70	0·29	0·643
4.9*b*	0·45	0·65	0·30	0·692
4.9*c*	0·45	0·60	0·33	0·750
4.9*d*	0·45	0·55	0·365	0·818
4·9*e*	1·20	0·70	1·19	1·71
4.9*f*	1·20	0·65	1·74	1·85
4.9*g*	1·20	0·60	2·36	2·00
4.9*h*	1·20	0·55	3·86	2·18

We now consider the regions within the dashed lines to contain the exact circuits of fig. 4.5 tuned by the parallel coils L_p of (4.22). The voltage transfer is still given by (4.26) which may be written as

$$\frac{E_L}{E_S} = 2\left(\frac{E_m}{E_S}\right)^2 \frac{R}{R_m}, \tag{4.37}$$

where E_m, E_L and E_S are the voltages shown in fig. 4.7. The voltage-transfer response can be written as a function of k_{15}, ζ, u and f/f_a as follows:

$$\frac{E_m}{E_S} = \frac{Z_1 Z_3}{R(Z_1 + Z_2 + Z_3) + Z_1(Z_2 + Z_3)}, \tag{4.38}$$

where

$$Z_1/a = \frac{j2k_{15}^2(\pi/2)\,f/f_a}{2k_{15}^2(\pi^2/8k_{15}^2 - 1) - \{(\pi/2)\,f/f_a\}^2},$$

$$Z_2/a = j\left\{\frac{2k_{15}^2}{(\pi/2)\,f/f_a} - \frac{2}{\tan\{(\pi/2)\,f/f_a\}}\right\}, \tag{4.39}$$

$$Z_3/a = \frac{j2\zeta \tan\{(\pi/2)\,f/f_a\}}{\zeta + j2 \tan\{(\pi/2)\,f/f_a\}}$$

and

$$R/a = \zeta/u.$$

The curves resulting from the computation of (4.37), (4.38) and (4.39) are presented in fig. 4.9*a* to *h*. In the graphs, the limits of the bandwidth, as defined in fig. 4.8, are indicated. The following facts may be concluded from these figures.

(a) The four cases with $\zeta = 0{\cdot}45$ (for which $\zeta/k_{15} < 1{\cdot}68$) give double-peaked responses, provided of course that the parallel coils L_p (eq. (4.22)) and the optimum value of R (given by u in fig. 4.8) are used in the external circuits. The case $\zeta/k = 0{\cdot}643$ gives a response characteristic which is not quite acceptable in the previously defined sense. The other four cases, for which $\zeta/k > 1{\cdot}68$, have single-peaked responses. These findings are in agreement with the predictions of fig. 4.8, a figure which itself was the result of approximate calculations.

(b) It is obvious that, for the delay-line-frequency response, the frequency f_a does not represent "the" central frequency. The minimum response (or, in the single-peaked case, the maximum response) does not occur at the frequency f_a; nor does f_a lie in the middle of the bandwidth.

(c) It is interesting to note that, as the computed graphs show, a larger value of k_{15} may not always be desirable: if $\zeta = 0{\cdot}45$ then a value for k_{15} of 0·70 is somewhat too high; this finding is confirmed by experiment.

The acoustic coefficient ϱ representing the amplitude of the reflected wave for a unit incident-wave amplitude, has also been computed. We have defined this coefficient in the same manner as it is done in transmission-line problems having a discontinuity in the line. Thus, this coefficient ϱ is the result of a one-dimensional approach. As was mentioned in the previous chapter, the reflected radiation in the DL1 actually consists of a part reflected by the transducers as well as of a part reflected at a glass-air interface. It is the former part that we are concerned with here. If the transducer be again shunted by L_p (eq. 4.22)) then ϱ is computed from

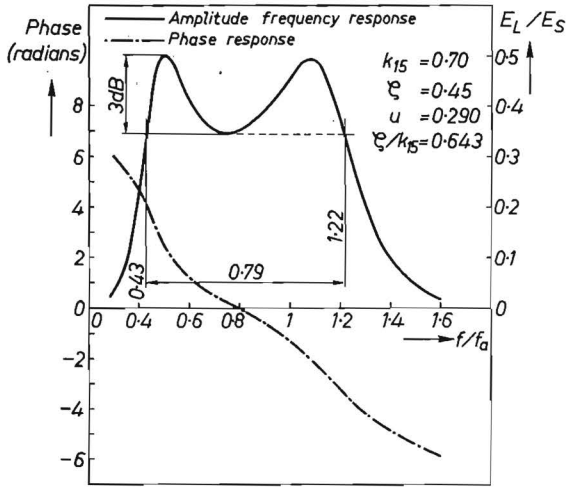


Fig. 4.9*a*.

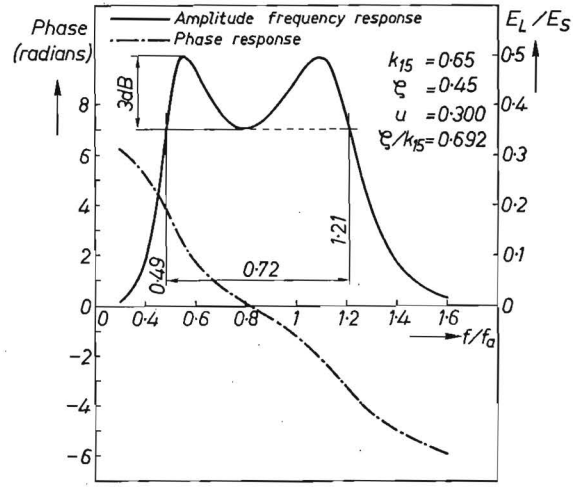


Fig. 4.9*b*.

Fig. 4.9. Computed transducer-pair responses.

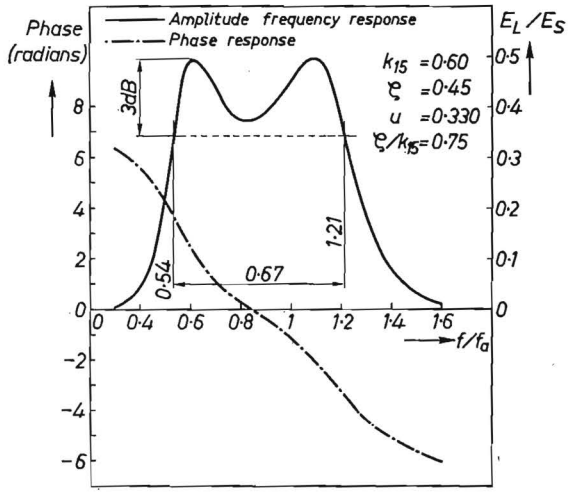


Fig. 4.9*c*.

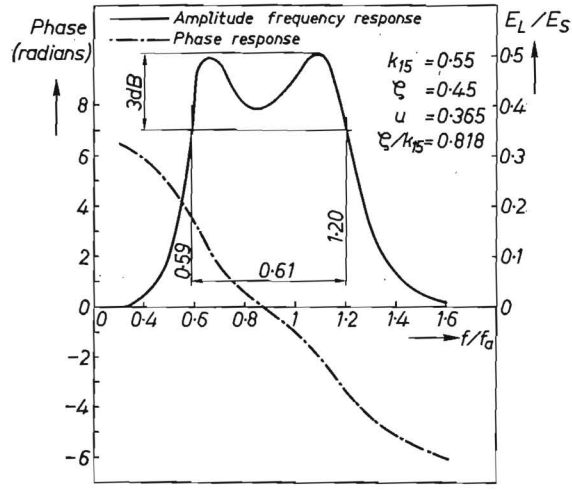


Fig. 4.9*d*.

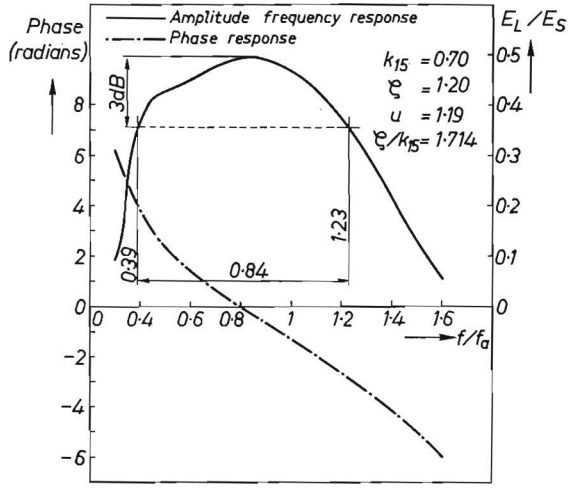


Fig. 4.9*e*.

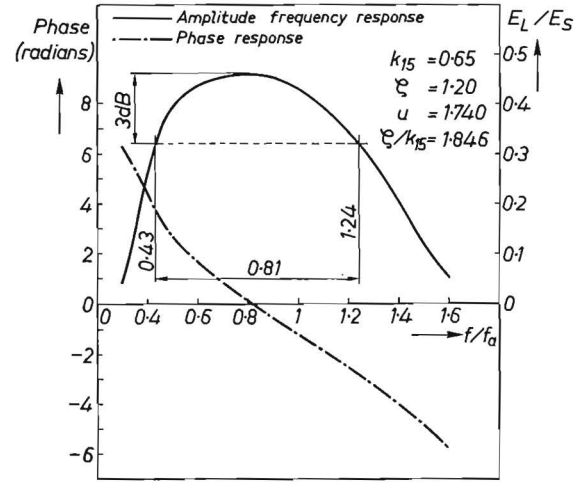


Fig. 4.9*f*.

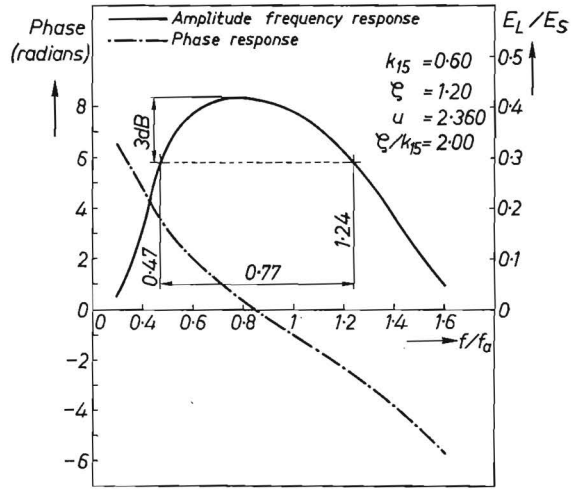


Fig. 4.9*g*.

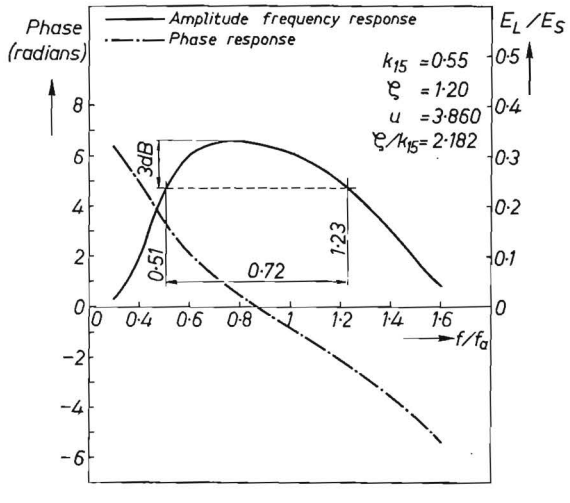


Fig. 4.9*h*.

$$\varrho = \frac{Z_T - \zeta}{Z_T + \zeta}, \tag{4.40}$$

where

$$Z_T = \frac{\left\{j2 \tan\left(\frac{\pi}{2}\frac{f}{f_a}\right)\right\}\left\{\frac{Z_2}{a} + \frac{(Z_1/a)\zeta/u}{Z_1/a + \zeta/u}\right\}}{j2 \tan\left(\frac{\pi}{2}\frac{f}{f_a}\right) + \frac{Z_2}{a} + \frac{(Z_1/a)\zeta/u}{Z_1/a + \zeta/u}} \tag{4.41}$$

and where Z_1/a and Z_2/a are given by (4.39). The reflection coefficient has been computed for the eight cases of table 4-I as well as for eight cases whose parameters are found by substituting $u = 1$ in the same table: $u = 1$ is the resistance ratio which, in the approximate treatment, made the reflection zero at the frequency $\omega_0'/2\pi$ (4.23). The computed graphs are shown in fig. 4.10.

4.4. Quantitative data on PXE3

For the transducer material PXE3 [4–10] — which is the material used in the DL1 delay line — we list and derive here several of the quantities which have been mentioned in the three previous sections. We choose dimensions which are approximately those used in the DL1; thus the thickness and the cross-section are $l = 0{\cdot}24.10^{-3}$ m and $A = 10^{-4}$ m^2. All quantities will be expressed in the Giorgi system.

We take from refs 4–7 and 4–10:

$$\begin{aligned} \varepsilon_{11}{}^{e} &= 500\ \varepsilon_0, \\ h_{15} &= 22.10^8\ \text{V/m}, \\ \varrho &= 7{\cdot}8.10^3\ \text{kg/m}^3. \\ k_{15} &= 0{\cdot}6. \end{aligned}$$

Values as high as 0·7 are quoted for k_{15}. The value actually obtained depends on the polarizing technique. We have chosen a lower value since, as we have just shown, a coupling factor of 0·7 is not even desirable in this particular case. Inserting these values in (4.15), (4.16) and (4.9) we find

$$\begin{aligned} \varepsilon_{11}{}^{\sigma} &= 781\ \varepsilon_0, \\ c_{44}{}^{D} &= 59{\cdot}5.10^9\ \text{kg m}^{-1}\,\text{s}^{-2}, \\ C_0{}^{S} &= 1844.10^{-12}\ \text{F}; \end{aligned}$$

eqs (4.3), (4.12) and (4.18) then give

$$\begin{aligned} V^D &= 2{\cdot}76.10^3\ \text{m/s}, \\ f_a &= 5{\cdot}75\ \text{MHz}, \\ a &= 32{\cdot}8\ \Omega. \end{aligned}$$

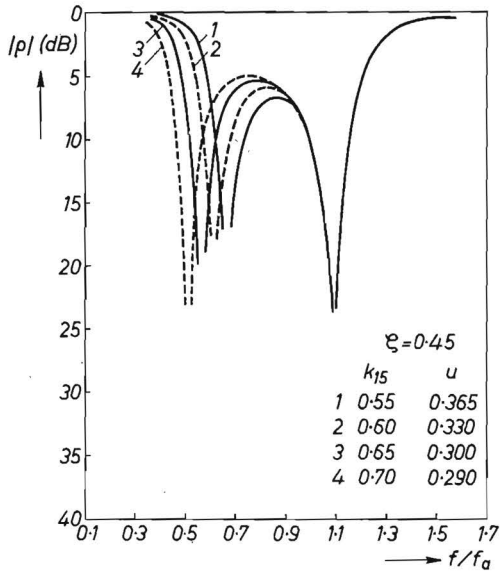


Fig. 4.10*a*.

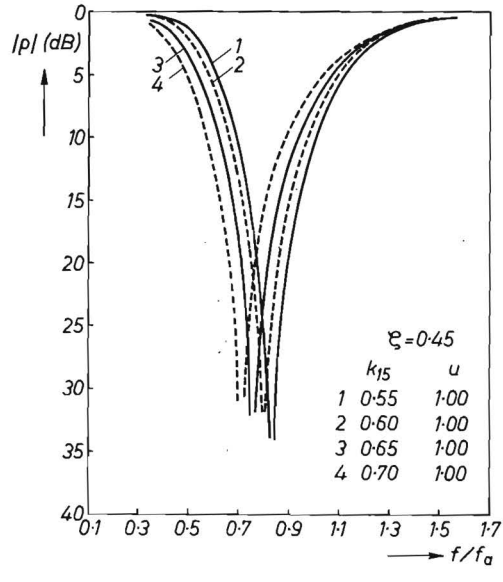


Fig. 4.10*b*.

Fig. 4.10. Reflection coefficient ϱ.

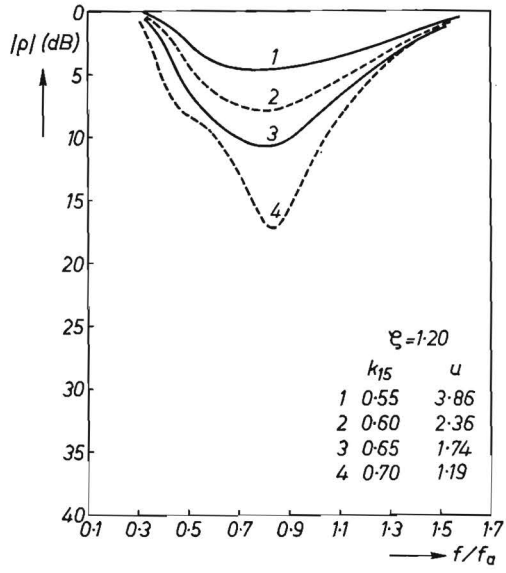


Fig. 4.10*c*.

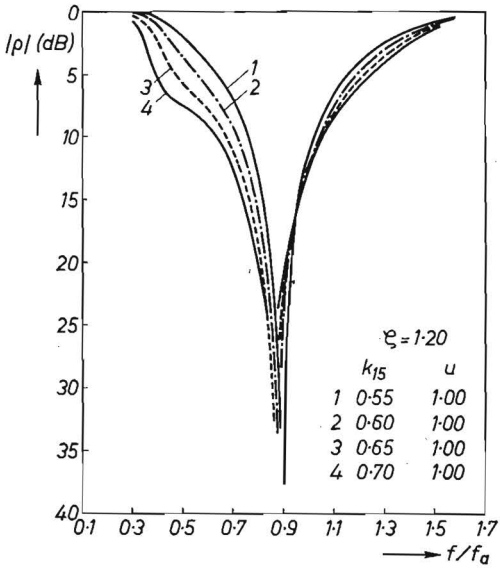


Fig. 4.10*d*.

Density and bulk shear-wave velocity in the potash-lead-silicate glass used for the propagation medium in the DL1 are $3{\cdot}73.10^3$ and $2{\cdot}58.10^3$, respectively. Thus

$$Z_2 = 9{\cdot}62.10^2 \text{ kg s}^{-1},$$

while (4.5) gives

$$Z_0 = 21{\cdot}5.10^2 \text{ kg s}^{-1}.$$

Hence

$$\zeta = 0{\cdot}45$$

and

$$\zeta/k_{15} = 0{\cdot}75.$$

The electrical equivalent of the radiating resistance of the propagation medium is found to be

$$R_m = 14{\cdot}7\ \Omega.$$

Figure 4.8 gives the optimum value of u of 0·33 for $\zeta/k_{15} = 0{\cdot}75$. This value of u has been used in the previous chapter. To conclude, we mention the values in the circuit of fig. 4.6:

$$\begin{aligned} L &= 1{\cdot}42\ \mu\text{H}, \\ f_0' &= 0{\cdot}844 f_a = 4{\cdot}85 \text{ MHz}, \\ C &= 746 \text{ pF}, \\ L_p &= 0{\cdot}576\ \mu\text{H}. \end{aligned}$$

4.5. Propagation

We conclude the chapter with a section on the propagation aspect of the DL1 delay line. If we deal less with this matter than with the transducer properties, it is not because the subject of propagation is considered less important; on the contrary, lack of phase linearity and unevenness of the amplitude-frequency response may be caused as much by the propagation of the line as by its transducer properties. We have however sought to design the DL1 in such a manner that the bandwidth limitation and the phase deviations are caused mainly by the transducers. Generally speaking this is obtained by choosing the lateral dimensions of the propagation material on the large side.

Although there exists a large amount of literature on wave propagation in structures of various geometries, it is probably correct to say that if very accurate knowledge is required for an actual delay-line structure, one usually needs to resort to the experimental investigation or to computations based on fundamental vibration equations.

In general, theoretical investigators have adopted two approaches. In the first approach, it is attempted to postulate modes of vibrations (usually propagation modes) and to find combinations of these modes that satisfy both the elastic-

wave equations and the boundary conditions. This problem generally becomes more difficult as the number of boundaries is increased. The geometry of the DL1 delay line may be described in a first approximation as a bar of rectangular cross-section, if we overlook the fact that the acoustic path is folded and, more important, that the guiding walls are rippled. Using the approach just mentioned, infinitely long bars of rectangular cross-section are reviewed by Meeker and Meitzler in a chapter of a recent series of books edited by Mason [4-11]). There seems to be no general exact solution for this case. Some incidental solutions are available; for example the Lamé modes [4-12]) which are valid for certain frequencies. Mindlin and Fox[4-13]) describe other solutions which hold at discrete frequencies and width-to-thickness ratios. All these solutions however do not apply in our case since they involve longitudinal modes and flexural modes in addition to shear modes. In short, this approach does not seem a promising one for any geometry which is more intricate than that of a strip line, or, at the most, a plate line. As representative for the second approach we refer to articles by Williams [4-14]), Stenzel [4-15]), Seki, Granato and Truell [4-16]), Bass [4-17]), Fujii and Yamada [4-18]). In general, the sending transducer is considered to be an equiphase surface; lateral dimensions are usually considered to be so large that the sending transducer (piston) is radiating into a semi-infinite medium. An attempt is made to find expressions for the field at points in the medium where the receiving transducer will be placed. The treatment is similar to that of a problem in optical-diffraction theory (Zwikker [4-19]), Born and Wolf [4-20]), Bouwkamp [4-21])). It is then assumed that the mechanical response of the receiving transducer is proportional to the integral of the field over its area.

The fact that this approach leads to a description of the field by one scalar — so that only one particle-movement direction is considered — is perhaps not a severe approximation for our case. If, once more, the DL1 is considered as a bar with rectangular cross-section, we notice: (a) the waves are SH waves — shear waves having particle-movement direction parallel to the boundary — for one pair of side boundaries, so that no mode conversion takes place upon reflection; (b) for the other pair of boundaries the waves are SV waves — shear waves whose particle-movement direction is in a plane through the boundary normal and the propagation direction — which, however, strike these boundaries so glancingly that again no mode conversion occurs. The particle movement is therefore expected to be mainly in one direction. A complication arises here since the boundaries of the DL1 are purposely rippled as this was experimentally shown to be advantageous; this means, however, that mode conversion may take place to some extent. It should be immediately added that the receiving transducer favours the reception of the desired vibration mode. This may be one of the mechanisms which can explain the response improvement obtained

by rippling: the boundaries remove part of the unwanted reflected radiation by conversion.

Nevertheless, if accurate prediction of the response is desired, it is usually not safe to ignore the role of the side boundaries completely. In a method of calculation followed by Sutton [4–22]) the basis is again the diffraction method, but the guiding boundaries are also taken into consideration; it is assumed that the radiation consists of rays for which the reflection laws of plane waves hold. Sutton considers SV waves, so that the Poisson ratio ν is needed to determine the phase change per reflection. The case studied by him is that of a very long plate. The method lends itself very well for use with a computer, although it might get intricate if a bar with rectangular cross-section were to be calculated in this way, since the number of mirror images would grow rather large. For the present writer several geometries were computed following the general method of Sutton, but using the formula (3.1) of the previous chapter. Figure 4.11*a* shows the amplitude- and group-delay characteristics. Characteristic dimensions were: plate thickness 8·35 mm and corresponding transducer size also 8·35 mm. In fig. 4.11*b* we show the output of one frequency broken down into several contributions each of these representing the output due to rays having undergone n reflections. Although these figures do not represent the case

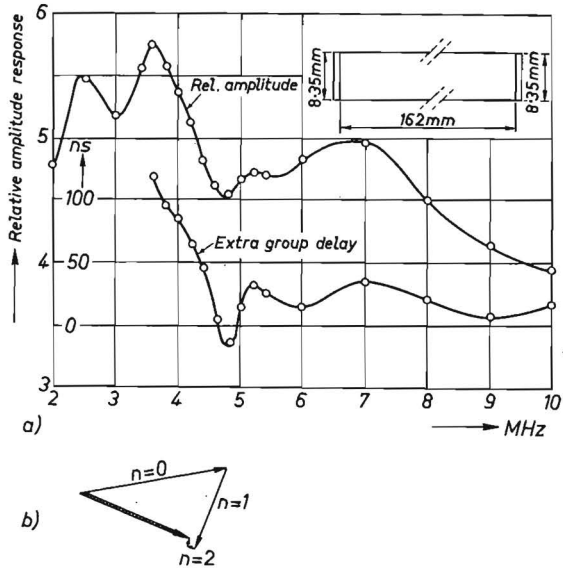


Fig. 4.11. Propagation of quasi shear-vertical waves in a plate. Rays for which $n \leqslant 6$ have been included in the computations; n is the number of reflections which a ray suffers between sending and receiving transducers. Plate material: glass 239 ($V_S = 2{\cdot}54$ km/s, $\nu = 0{\cdot}23$). Plate and transducer dimensions: as in fig. *a*.
(*a*) Computed amplitude response and computed extra group delay.
(*b*) Contributions of rays suffering n reflections; $f = 4{\cdot}4$ MHz.

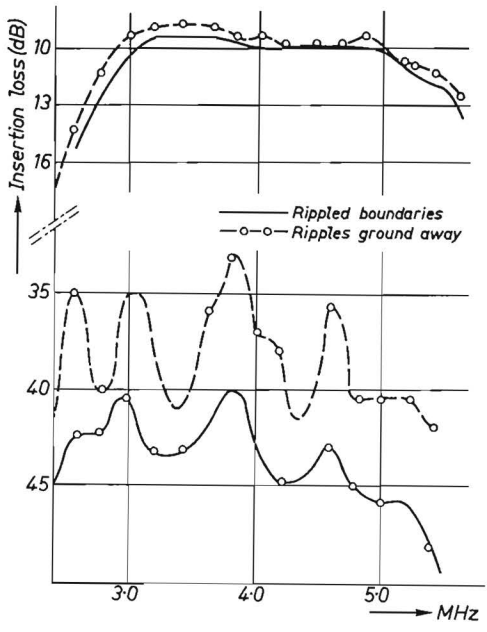


Fig. 4.12. Measured effect of rippling.

of the DL1 delay line, they allow us to reach conclusions. First, the findings of Sutton may not be translated for use in the case of the DL1. For example his conclusion that "no significant energy is translated directly along the path usually thought of as the 'straight through' path" clearly does not hold here. The reason why this statement does apply in Sutton's case is that his line is much longer, with the result that, there, in the neighbourhood of $n = 0$, one has a succession of small contributions of practically equal amount and differing 180° in phase. Second, and more important, fig. 4.11*b* indicates that, even when the significant dimensions of plate and transducer are as much as 8·35 mm, it cannot very well be said that the boundaries do not play a role. The effect of rippling the side boundaries has been determined experimentally. Figure 4.12 shows the insertion-loss vs frequency curves for a sample of a normal PAL line and for a line which was obtained by grinding away the ripples of the same sample. It is seen that the main output signal is not much improved but a worthwhile suppression of the 3τ reflections is obtained. The fact that the latter signals are influenced more can be explained by noting that the delay line is two or three times "longer" for reflections. The fact that the main signal is influenced so little may be taken as an indication that the lateral dimensions of the DL1 are large enough, so that the propagation is a small factor in the overall response.

REFERENCES

4–1) C. Zwikker, Fysische Materiaalkunde, Wetenschappelijke Uitgeverij N.V., Amsterdam, 1966.
4–2) Document U.I.P. 11 (S.U.N. 65-3), 1965.
4–3) Standards on piezoelectric crystals 1949, 49I.R.E.14.S1 or Proc. I.R.E. **37**, 1378-1395, 1949.
4–4) I.R.E. Standards on piezoelectric crystals — The piezoelectric vibrator: definitions and methods of measurement, 1957, 57I.R.E.14.S1 or Proc. I.R.E. **45**, 353-358, 1957.
4–5) I.R.E. Standards on piezoelectric crystals: Determination of the elastic piezoelectric and dielectric constants — The electromechanical coupling factor, 1958, 58I.R.E.14.S1 or Proc. I.R.E. **46**, 764-778, 1958.
4–6) I.R.E. Standards on piezoelectric crystals: Measurements of piezoelectric ceramics, 1961, 61I.R.E.14.S1. or Proc. I.R.E. **49**, 1161-1169, 1961.
4–7) C. F. Brockelsby, J. S. Palfreeman and R. W. Gibson, Ultrasonic delay lines, London Iliffe Books Ltd., 1963.
4–8) H. E. Müser and H. Bittel, Arch. elektr. Übertr. **9**, 231-236, 1955.
4–9) R. Bechmann, Arch. elektr. Übertr. **9**, 122-130, 1955.
4–10) Piezoxide and PXE are trademarks of the N.V. Philips' Gloeilampenfabrieken, Eindhoven. See also the Bulletin "Piezoxide" edited by the Philips Industrial Components and Materials Division, May 1963.
4–11) W. P. Mason (ed.), Physical acoustics, Methods and devices, Academic Press, New York, London, Vol. I, Part A.
4–12) G. Lamé, Leçon sur la théorie mathématique de l'élasticité des corps solides, Gauthiers-Villars, Paris, 1866.
4–13) R. D. Mindlin and E. A. Fox, J. appl. Mech. **27**, 152-158, 1960.
4–14) A. O. Williams Jr, J. acoust. Soc. Am. **23**, 1-6, 1951.
4–15) H. Stenzel, Acustica **2**, 263-281, 1952.
4–16) H. Seki, A. Granato and R. Truell, J. acoust. Soc. Am. **28**, 230-238, 1956.
4–17) R. Bass, J. acoust. Soc. Am. **30**, 602-605, 1958.
4–18) Y. Fujii and K. Yamada, J. acoust. Soc. Am. **40**, 249-251, 1966.
4–19) C. Zwikker, Leerboek der optiek, P. Noordhoff N.V., Groningen-Batavia, 1933.
4–20) M. Born and E. Wolf, Principles of optics, Pergamon Press, 1959, p. 379.
4–21) C. J. Bouwkamp, J. Math. and Phys. **26**, 79, 1947.
4–22) P. M. Sutton, J. acoust. Soc. Am. **31**, 34-43, 1959.

5. MEASUREMENTS

This chapter discusses the methods of measuring the main electrical characteristics, the requirements for which have been examined in chapter 2. Measurements of ultrasonic properties such as the velocity of the acoustic waves, or the attenuation of the medium, are not discussed; for general information on such subjects, the reader is referred to articles by McSkimin [5-1,2]) Bolef and De Klerk [5-3]) and Fraser and LeCraw [5-4]).

5.1. Insertion loss, bandwidth, reflections

The insertion loss (I.L.) of a device is given by

$$\text{I.L.} = 10 \log_{10} \frac{P_1}{P_2},$$

where P_1 is the power delivered to the load resistance R_L when it is connected directly to the source (of resistance R_S), while P_2 is the power delivered to R_L when the device is inserted between load and source. We have chosen R_S and R_L to be 150 Ω each and the two shunt coils are considered to be part of the "device". The I.L. may be measured by an inexpensive and accurate circuit described by Meitzler [5-5]) and schematically shown in fig. 5.1. The measuring signal is fed to the delay line as well as to a calibrated attenuator. By operating the switch, it is possible to display either the output of the delay line or the attenuated signal. The two signals are made equal in amplitude by means of the attenuator. It can be shown that if R_S and R_L are the resistances between which it is desired to know the insertion loss, if

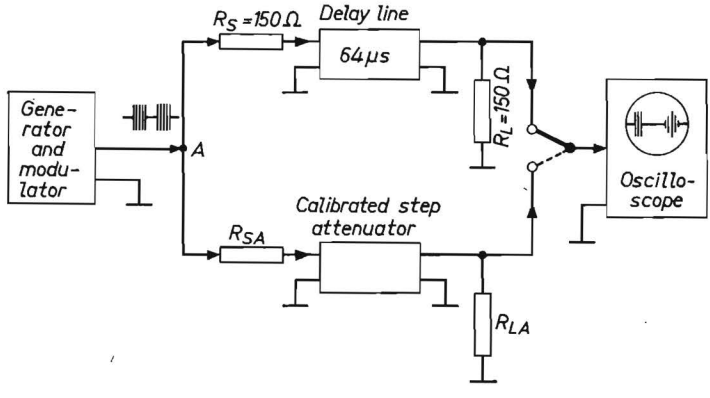


Fig. 5.1. Block schematic arrangement for insertion-loss measurements; R_{LA} = image impedance of attenuator.

$$\frac{R_{SA}}{R_{LA}} = \frac{R_S}{R_L},$$

where R_{LA} is the iterative impedance of the calibrated attenuator, and if — for the special case that we are measuring reflections — the driving-source impedance is zero, then this attenuator reads the value of the I.L. directly.

If continuous sine waves are employed as measuring signal, the I.L.-frequency curve may be obtained by making a number of measurements at different frequencies; the bandwidth may then be determined by finding the 3-dB down points. It can be shown that in this case the provision that the driving-source impedance be zero is not needed. By using an r.f. burst as the measuring signal, it becomes possible to display — and thus to measure — the main response and the reflections of the delay line. The pulse duration should be long enough, so that it is not the amplitude- and phase-response limitations which are being measured. The pulse-repetition frequency should be low enough so that multiple travel signals from the delay line will have died down before a next burst. If the main output pulse (1τ pulse) is measured in this way the source impedance may again have any value; but it should be zero if 2τ or 3τ pulses are measured. That this is so can be understood by realizing that if this impedance is not zero, then there may be signals at A which contribute to 2τ or 3τ signals, but which do not contribute to the selected attenuator output signal.

5.2. Phase and group delay, temperature stability of phase response, phase adjustment by grinding

We define the phase response β with the aid of fig. 5.2; it is the phase difference between the phase of the voltage across the load resistance (E_L) and that of the source voltage (E_S); alternatively β is the phase difference between E_L and I (fig. 5.2*b*). Thus, the delayed signal is E_L while the direct signal is identified with E_S (or I), not with E_i.

A schematic diagram of a circuit for determining whether the delay line satis-

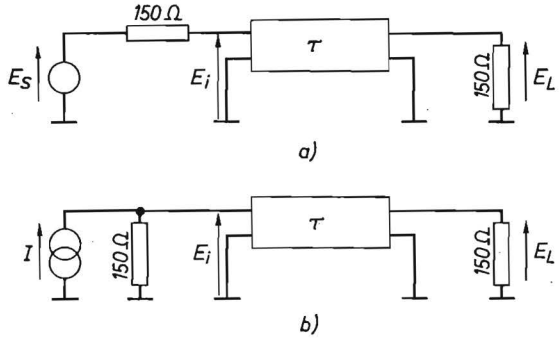


Fig. 5.2. Definition of phase delay.

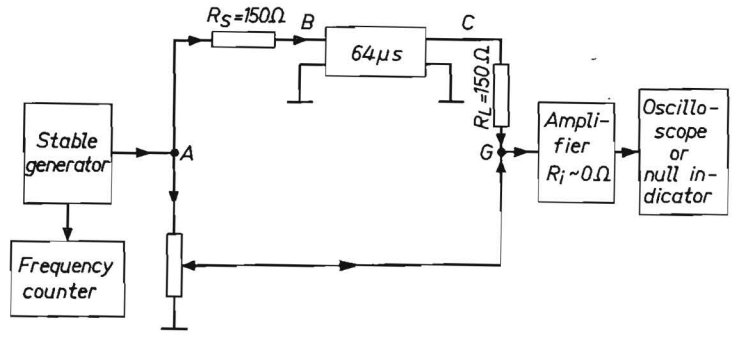


Fig. 5.3. Block schematic arrangement for phase-delay measurements.

fies the phase-response requirement, is shown in fig. 5.3. The direct signal (at A) is compared in phase with the delayed signal, by adding the two — after having them equalized in amplitude by means of the potentiometer — at the low-impedance point G. If the oscilloscope indicates the sum signal to be zero, then the phase response equals $(2m + 1)\pi$ where m is any integer. In this case we have considered the current through R_L rather than the voltage across it, as the delayed signal.

The continuous-wave generator needs to be fairly stable so that the frequency stays sufficiently constant during one measurement. It also needs to be capable of fine adjustment. Since a variation of approximately 60 Hz corresponds to a phase-delay time of 1 ns, the generator should allow frequency adjustment to within some 10 Hz.

The circuit of fig. 5.3 can be used also for the measurement of the group-delay time. For this measurement the frequency difference $f_2 - f_1$ for two adjoining "zeros" (phase cancellations) is noted: the average group delay within the frequency range f_1 to f_2 then equals $1/(f_2 - f_1)$.

For the measurement of the phase-response variation with temperature the principle of fig. 5.3 can again be used. The delay line will be placed in an oven. The required accuracy and stability of the measuring equipment are higher than in the case of the phase-response measurement. Since the whole range of the variation which is going to be measured is no more than a few nanoseconds, a measuring sensitivity of 0·1 nanosecond is wanted. The equipment stability should be high since the measurements are time-consuming. They may last hours if the conditions in a television set are simulated; or they may last weeks if one investigates how long the after-effects in the media last. The author has obtained good results with the arrangement of fig. 5.4. The purpose of course is again phase cancellation of the currents at G. For an arbitrary delay line this can always be realized by introducing a phase shifter (0-180°) of the correct wave impedance either at F or at D. But if it is desired to measure a DL1 delay

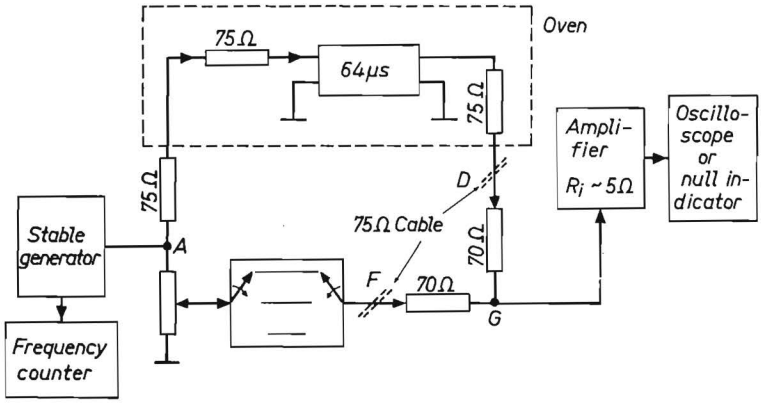


Fig. 5.4. Measurement of phase-delay variation with temperature.

line — which is adjusted to give phase opposition with the direct signal — the phase-delay difference to be made up is only a few nanoseconds. This is done in a simple and stable way by adding the necessary amount of cable, of the correct wave impedance, at F or at D. Measuring is accomplished by substitution: if the phase delay of the delay line changes as a result of the temperature change, the phase cancellation is restored by substituting an equal amount of phase change in the bottom branch. This may be done by operating the variable phase delay shown, a crude but effective device made for the purpose at the laboratory. It is a box containing a number of cables increasing in length by steps of 0·1 nanosecond; a switch allows the selection of the cable needed.

Since the effect of a phase-delay change of 0·1 nanosecond is equal to that of a change in measuring frequency of approximately 6 Hz, it follows that the generator must be adjustable to within about 1 Hz. The factors contributing to a sensitive zero indication are: a sensitive amplifier, absence of noise and absence of non-linear distortion. Noise and distortion can easily be kept small since the measurement is done at one frequency.

The arrangement has the following advantages. It contains only passive elements within the two measuring branches; these can be made very stable, so that the variations measured are those due to the delay line, its transducers and associated coils. The cables at D and F may be as long as desired, which facilitates precise phase opposition.

During one of the final stages of fabrication of the DL1, that is, after the transducers have been mounted, the wiring applied and shunt coils connected and tuned, the required delay adjustment is obtained by grinding the reflection facet of the glass while electrically monitoring the delay time. The phase measurement gives a multiple-valued result and so it has to be preceded by a group-delay measurement. This does not need to be performed by the rather involved

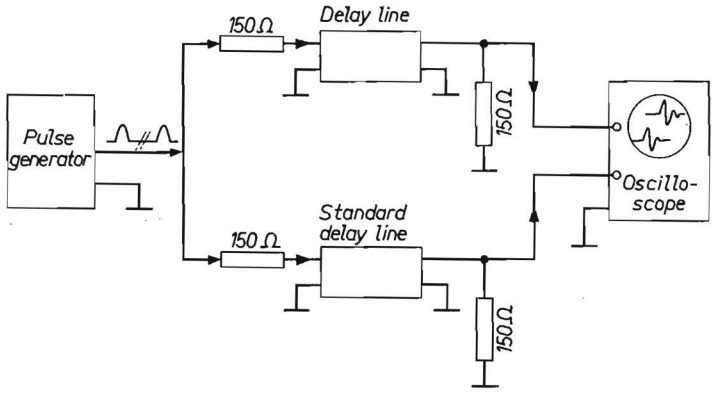


Fig. 5.5. Coarse group-delay measurement.

method described above. A simple method is shown in fig. 5.5. Here the pulse-delay time of the line to be adjusted is compared with that of a standard line receiving the same pulse at its input. The oscilloscope used is one of the kind which can display two signals on a common horizontal time base. The delay difference shows up as a difference in the horizontal position of the two traces. If higher accuracy were required it would be possible to use r.f. pulses — instead of the video pulses shown — and subsequent demodulation. This would produce a less distorted output pulse.

To conclude, we mention that the measurement techniques described are typically laboratory solutions. They have the dependability and absolute accuracy which often goes with simplicity; to obtain, in addition to accuracy, the speed and automatic operation which are needed in production, more complex equipment is usually needed.

REFERENCES

[5-1]) H. J. McSkimin, J. acoust. Soc. Am. **22**, 413-418, 1950.
[5-2]) H. J. McSkimin, J. acoust. Soc. Am. **33**, 606-615, 1961.
[5-3]) D. I. Bolef and J. de Klerk, I.E.E.E. Trans. **UE-10**, 19-26, 1963.
[5-4]) D. B. Fraser and R. C. LeCraw, Rev. sci. Instr. **35**, 1113-1115, 1964.
[5-5]) A. H. Meitzler, I.R.E. Trans. **PGUE-6**, 1-16, 1957.

Dankbetuiging

Het in dit proefschrift beschreven onderzoek werd uitgevoerd in het Natuurkundig Laboratorium der N.V. Philips' Gloeilampenfabrieken. Veel dank ben ik verschuldigd aan de directie van dit laboratorium, in het bijzonder aan Dr. J. Haantjes en aan Dr. Ir. A. E. Pannenborg voor de mij geboden gelegenheid het onderzoek te verrichten en in de vorm van een proefschrift te publiceren.

Ik betuig mijn dank aan G. J. Lubben en Dr. F. W. de Vrijer voor hun waardevolle adviezen en voor het kritisch doornemen van mijn manuscript. Ik dank C. M. van der Burgt voor zijn opbouwende kritiek.

Met erkenning maak ik gewag van de daadwerkelijke steun die ik van velen buiten het Natuurkundig Laboratorium mocht ontvangen. H. Hoeve dank ik voor de enthousiaste wijze waarop hij het vele werk in het laboratorium voor zijn rekening nam.

Samenvatting

Het PAL kleurentelevisietransmissiesysteem is een van de twee in Europa ingevoerde transmissiesystemen. PAL kleurentelevisieontvangers zijn in het algemeen toegerust met ultrasone vertragingslijnen die dienen om electrische signalen een vertraging van 64 μsec — de periode van de horizontale aftastfrequentie — te laten ondergaan. Een aantal problemen, verband houdende met deze vertragingslijn worden in dit proefschrift behandeld. Een ultrasone vertragingslijn voor PAL ontvangers werd ontwikkeld; deze wordt verder aangeduid als type DL 1.

Na een algemene introductie (hoofdstuk 1) wordt, in hoofdstuk 2, allereerst de rol beschreven welke de vertragingslijn vervult in de PAL ontvanger. Te dien einde worden de grondslagen van het PAL transmissiesysteem kort gereleveerd. Het is mogelijk PAL kleurentelevisiesignalen te ontvangen in een ontvanger die niet uitgerust is met een vertragingslijn van het hier bedoelde type (PAL-s ontvanger). De nadelen, die het gevolg kunnen zijn van deze wijze van ontvangst, worden beschreven. In het bijzonder wordt uiteengezet dat de visuele uitmiddeling, die een voorwaarde is voor goede PAL-s ontvangst, in feite niet plaats vindt wanneer het oog mee beweegt met de schijnbare opwaartse beweging van het stoorpatroon dat in de literatuur bekend is onder de naam „Hannover bars".

Vervolgens worden de eisen, die het PAL transmissiesysteem stelt aan de vertragingslijn, onderzocht. Bepaald worden onder meer de noodzakelijke normen en toleranties betrekking hebbende op de phaseresponsie bij de kleurenhulpdraaggolf, de frequentiekarakteristiek en de phasekarakteristiek. Verschillende vertragingseigenschappen dienen in hoge mate onafhankelijk te zijn van temperatuursvariaties. Besproken worden de effecten die het gevolg zijn van reflecties. De gevonden normen en toleranties zijn samengevat in tabel 2-I.

In hoofdstuk 3 wordt afgeleid, hoe men tot de keuze van de ontwikkelde vertragingslijn (type DL 1) kan komen. Hiertoe wordt, behalve dit type, ook een aantal alternatieve constructies besproken. Een dergelijke behandeling komt voor een deel neer op een beschrijving van de stand van de techniek. Uit het vergelijkend onderzoek volgt, dat a priori twee types vertragingslijn voor toepassing in aanmerking zouden kunnen komen. In verband met de huidige stand van de techniek is het ontworpen type te preferen. Het hoofdstuk wordt beeindigd met een gedetailleerde discussie van de eigenschappen van de DL 1. Nagegaan wordt in de eerste plaats in hoeverre deze eigenschappen voldoen aan de in hoofdstuk 2 gevonden eisen. Enige aandacht wordt ook besteed aan de verdeling van de verliezen. De factoren die invloed hebben op de reflecties worden onderzocht; in het bijzonder wordt er de aandacht op gevestigd dat een eendimensionale theorie niet in staat is de reflectie-eigenschappen van de DL 1 te beschrijven.

Hoofdstuk 4 is hoofdzakelijk gewijd aan berekeningen van verschillende overdrachtseigenschappen van paren van transducenten. De resultaten van numerieke berekeningen worden in de vorm van grafieken gepresenteerd. Vooraf worden de benodigde formules afgeleid. Er zijn, ook als men geen rekening houdt met de voortplantingseigenschappen in het vertragingsmedium, vrij veel parameters waarover men beschikken kan en welke het gedrag van de bedoelde overdrachtseigenschappen bepalen. Om te voorkomen dat het aantal gevallen dat men numeriek wenst te berekenen, onhandelbaar groot wordt, is het gewenst het aantal onafhankelijk van elkaar te kiezen parameters te beperken. Een relatie tussen de parameters wordt gevonden uit de enigermate arbitraire bepaling dat de bandbreedte maximaal dient te zijn. De bedoelde relatie is weergegeven in fig. 4.8 en is analytisch gevonden uit een vereenvoudigd equivalent circuit dat ook vooraf afgeleid is. Gebruik makend van deze relatie worden dan acht gevallen (tabel 4-I) gekozen voor numerieke berekening van de frequentie- en fasekarakteristieken. Reflectiecoefficienten worden numeriek berekend voor dezelfde acht gevallen, waaraan toegevoegd worden acht gevallen, die volgens de eerder gegeven benaderende behandeling een kleinere reflectiefactor voor centrale frequenties zou moeten vertonen. Het hoofdstuk eindigt met een beschouwing over voortplantingseigenschappen. Men kan, voor het geval van de vertragingslijn van het type DL 1, aannemelijk maken dat de bandbreedtebeperking veel meer bepaald wordt door de eigenschappen van de transducenten en door de waarden van de electrische belastingselementen, dan door de voortplantingseigenschappen van de lijn.

Hoofdstuk 5 tenslotte behandelt de methodes waarmede in het laboratorium de belangrijkste vertragingslijneigenschappen gemeten werden.

Levensbericht

29 juli 1921	:	Geboren te Rotterdam
1940	:	Eindexamen H.B.S.-B, 's-Gravenhage
1948	:	Ingenieursexamen natuurkunde Technische Hogeschool Delft, afgestudeerd bij Prof. Dr. R. Kronig
1948-1954	:	Development Engineer, Eastman Kodak Company, Rochester N.Y., U.S.A.
1954-1955	:	Senior Scientist, University of New York N.Y., U.S.A.
1955-1968	:	Wetenschappelijk medewerker, Natuurkundig Laboratorium, N.V. Philips' Gloeilampenfabrieken, Eindhoven.
1968-heden	:	Leider ontwikkeling, Industrie Groep „Electronic Distribution Systems", onderdeel van de Hoofd-industriegroep Radio, Grammofoon en Televisie, N.V. Philips' Gloeilampenfabrieken, Eindhoven

STELLINGEN

I

Als definitie voor het begrip groeplooptijd van een netwerk kan dienen de uitdrukking $d\varphi/d\omega$, waarin φ de phaseresponsie van het netwerk en ω de hoekfrequentie voorstellen. Bij de hantering van deze uitdrukking beschouwt men altijd een zeker frequentieinterval. Het is van belang er rekening mede te houden dat men bij de afleiding van deze uitdrukking aangenomen heeft dat de amplituderesponsie binnen het beschouwde frequentieinterval constant is.

II

Voor een enkele willekeurig gekozen frequentie kan men de reflecties, die in het algemeen optreden in ultrasone vertragingslijnen, elimineren, ook al zijn de mechanische impedanties van propagatiemateriaal en transducent materiaal niet aan elkaar gelijk.

Dit proefschrift, § 3.6.1.

III

De impedanties waarmede een ultrasone vertragingslijn extern afgesloten dient te worden om maximale bandbreedte te verkrijgen, zijn niet gelijk aan de afsluitimpedanties welke benodigd zijn voor het verkrijgen van minimale reflecties voor frequenties in het midden van de doorlaatband.

Dit proefschrift, § 4.2.

IV

Ofschoon het voor de transducenten van ultrasone vertragingslijnen toegepaste materiaal in het algemeen een hoge electromechanische koppelfactor dient te bezitten kan onder bepaalde omstandigheden deze factor ook te hoog zijn.

Dit proefschrift, § 4.3.

V

Ontvangt men PAL kleurentelevisiesignalen met een kleurentelevisieontvanger welke niet voorzien is van een decodeerder met vertragingslijn, dan kunnen, zoals bekend is, differentiële phasefouten in de overdrachtsweg of in de ontvanger, aanleiding geven tot een zich in verticale richting bewegend patroon van horizontale lijnen. De verrassend grote zichtbaarheid van dit storende patroon kan voor een belangrijk deel hieruit verklaard worden dat de visuele uitmiddeling, welke een stilstaand oog zou kunnen effectueren, te niet gedaan wordt door het medebewegen van het oog met de lijnenstructuur.

VI

De door J. J. Went afgeleide formule voor de tunnelweerstand van een elektrisch contact vertoont niet de juiste fysische dimensie.

J. J. Went, Philips Technisch Tijdschrift **5** ,249-254, 1940.

VII

De ontwikkeling van goede en goedkope niet-professionele apparatuur voor televisieregistratie op magnetische band wordt ernstig belemmerd door het ontbreken van een aftastmechanisme zonder mechanische traagheid.

VIII

Brown komt, in zijn afleiding van de mechanische spanningen in een magnetisch lichaam tot een onjuiste formule. Ten onrechte neemt hij aan dat de ponderomotorische krachten loodrecht op het oppervlak staan.

W. F. Brown, Rev. mod. Phys. **25**, 131. 1953

IX

Het is gewenst dat het S.U.N. comité (Commission for Symbols, Units and Nomenclature) van de I.U.P.A.P. (International Union of Pure and Applied Physics) haar normalisatiewerkzaamheden uitstrekt tot de kruisgebieden van de wetenschap.

X

Het verdient aanbeveling, de leerlingen van het voorbereidend wetenschappelijk onderwijs onderricht te geven in de beginselen van niet-euclidische meetkunde, opdat zij enig inzicht verkrijgen in axiomastelsels.